First insights into the dynamic protein changes in goat Semitendinosus muscle during the post-mortem period using high-throughput proteomics

Melisa Lamri, Antonella Della Malva, Djamel Djenane, Marzia Albenzio, Mohammed Gagaoua

First insights into the dynamic protein changes in goat *Semitendinosus* muscle during the *post-mortem* period using high-throughput proteomics

Melisa Lamri [1], Antonella della Malva [2], Djamel Djenane [1], Marzia Albenzio [2] and Mohammed Gagaoua [3,*]

[1] Laboratoire de Qualité et Sécurité des Aliments, Université Mouloud Mammeri, Tizi-Ouzou 15000, Algeria

[2] Department of Agriculture, Food, Natural Resources and Engineering (DAFNE), University of Foggia, 71121 Foggia, Italy

[3] PEGASE, INRAE, Institut Agro, 35590 Saint-Gilles, France

* Corresponding author: mohammed.gagaoua@inrae.fr

Abstract

Proteomics plays a key and insightful role in meat research in the post-genomic era. This study aimed to unveil using a shotgun proteomics approach the temporal dynamic changes in early post-mortem proteome of goat *Semitendinosus* muscle. Therefore, the evolution and comparison of the muscle proteome over three post-mortem times (1, 8 and 24 h) was assessed. The temporal proteomics profiling quantified 748 proteins, from which 174 were differentially abundant (DAPs): n=55 between 1h *versus* 8h; n=52 between 8h *versus* 24h and n=154 between 1h *versus* 24h. The DAPs belong to myriad interconnected pathways. Binding, transport and calcium homeostasis, as well as muscle contraction and structure exhibited an equivalent contribution during post-mortem, demonstrating their central role. Catalytic, metabolism and ATP metabolic process, and proteolysis were active pathways from the first hours of animal bleeding. Conversely, oxidative stress, response to hypoxia and cell redox homeostasis along chaperones and heat shock proteins accounted for the large proportion of the biochemical processes more importantly after 8h post-mortem. Overall, the conversion of muscle into meat is largely orchestrated by energy production as well as mitochondrial metabolism and homeostasis through calcium and permeability transition regulation. The study further evidenced the role of ribosomal proteins in goat post-mortem muscle, signifying that several proteins experiencing changes during storage, also undergo splicing modifications, which is for instance a mechanism known for mitochondrial proteins. Overall, temporal proteomics profiling of early post-mortem muscle proteome offers an unparalleled view of the sophisticated post-mortem biochemical and proteolytic events associated with goat meat quality determination.

Keywords: Goat muscle proteome; Meat tenderization; Biological processes; Muscle structure; Energy metabolism; Apoptosis, Oxidative stress; Biomarkers; Proteasome; Ribosomal proteins.

1. Introduction

The conversion of muscle into meat, also known as meat tenderization, is a complex process involving a combination of sophisticated cascade of biochemical, energetic and physical events occurring during cold storage of carcasses and during retail/display of meat cuts (Hopkins & Ertbjerg, 2023; Ouali et al., 2013). The study of the underlying mechanisms behind the tenderization phases of meat has fascinated researchers for the past decades (Hopkins & Geesink, 2009; Hopkins & Thompson, 2001; Ouali, 1990; Purslow, Gagaoua, & Warner, 2021; Wicks et al., 2022), who ascribed such mechanisms to be partly related to the endogenous proteolytic systems (proteolysis) through the modifications they induce in the muscle structure, thereby playing key roles in the determination of the final meat quality (Kemp, Sensky, Bardsley, Buttery, & Parr, 2010; Matarneh, Scheffler, & Gerrard, 2023; Ouali et al., 2013). In fact, the changes during the post-mortem period in both the structure and status of muscle proteins along with their spatial arrangements due to the physicochemical and enzymatic reactions are pivotal events defining the development of meat quality traits (Gagaoua, Duffy, et al., 2022; Hughes, Oiseth, Purslow, & Warner, 2014). However, our knowledge is still very limited, especially for some species such as goat, and several aspects of meat tenderization phases even in other species on the interplay of apoptosis and autophagy, are not yet fully elucidated.

Because of the importance of the conversion of muscle to meat at the onset of the animal's death, there is significant interest in developing strategies to decipher and thoroughly characterize such events with the goal of reducing variability and consistently improving the overall eating quality of meat. Therefore, the application of high-throughput sequencing methods in the frame of foodomics has been used extensively nowadays and has allowed, over the last two decades, to reveal the involvement of several molecular signatures (Gagaoua, Terlouw, et al., 2021), thereby leading to a better understanding of the mechanisms that govern the determination of several meat quality traits (D'Alessandro & Zolla, 2013; della Malva, Maggiolino, et al., 2022; Munekata, Pateiro, López-Pedrouso, Gagaoua, & Lorenzo, 2021; Purslow et al., 2021). With the omics technological developments and the emergence of several computational and statistical tools and models, proteomics has evolved rapidly over the past decades. Further, it was hugely adopted by meat scientists and allowed an in-depth understanding of the current and emerging meat research questions namely in deciphering the unknowns related to the conversion of muscle into meat and for the discovery of biomarkers (Gagaoua & Picard, 2022; Gagaoua, Schilling, Zhang, & Suman, 2022). Indeed, proteins form a fundamental part of muscle structure and

participate in all cellular reactions, with substantial dynamic changes occurring since the first minutes post-slaughter (X. Jia et al., 2007; X. Jia, Hollung, Therkildsen, Hildrum, & Bendixen, 2006). The dynamic changes of proteins could regulate muscle functions like enzyme activity, protein stability and degradation, and even muscle contraction, all of which are involved in post-mortem changes in muscle and meat quality determination (D'Alessandro & Zolla, 2013; Ouali et al., 2013). Thus, the application of proteomics is a great way to unravel the huge complexity of the muscle proteomes (or sub-proteomes) by the analyses of the complete or partial set of proteins present in muscle, their structure, expression, modifications along the interactions with other molecules (López-Pedrouso, Lorenzo, Gagaoua, & Franco, 2020; Munekata et al., 2021; Picard & Gagaoua, 2020; Purslow et al., 2021; Verónica Sierra et al., 2021). For example, proteomics was successfully used to propose explanatory mechanisms at the origin of the variability of different eating qualities of meat from many species and also to propose biological markers (della Malva, Gagaoua, et al., 2022; Gagaoua, Bonnet, Ellies-Oury, De Koning, & Picard, 2018; Gagaoua, Terlouw, et al., 2021; Gagaoua, Troy, & Mullen, 2021; Munekata et al., 2021; Verónica Sierra et al., 2021). However, to the best of our knowledge, no study has yet examined the dynamic changes occurring in the early post-mortem muscle proteome of goat meat. Thus, this study aimed for the first time to decipher those changes in *Semitendinosus* muscle of Saanen x *Naine de Kabylie* crossbred goats raised in an extensive system in Kabylia Mountains (North of Algeria). *Naine de Kabylie* breed is an indigenous goat that is mainly found in the Kabylia Mountains and generally raised for the production of meat which is appreciated by the consumers (Lamri, Djenane, & Gagaoua, 2022). It is characterized as robust and of small size: 65 ± 2 cm for the males and 62 ± 2 cm for the females, with respective weights of 60 ± 3 kg and 47 ± 2.5 kg. The body of *Naine de Kabylie* breed is elongated with a straight and rectilinear top, the head is thin and carries horns directed towards the back, the color of the dress is variable, but the dominant colors are: white, red, beige, red piebald and black. Its ears are small and pointed for the subjects with white coat, and medium long for the subjects with beige coat. Finally, its hair is ranging from 3 to 9 cm. This study also aims to reveal, through label-free shotgun proteomics and bioinformatics approaches, the molecular signatures underlying the conversion of muscle into meat and the key interacting protein biomarkers.

2. Materials and Methods

2.1. Goats and slaughtering procedure

All the experimental procedures used in this trial were in compliance with the Algerian guidelines for the care and use of animals. The animal study protocol was approved by the Ethics Committee of the Université Mouloud Mammeri, Tizi-Ouzou (Algeria) as previously described (Lamri et al., 2023). The experiment included eight young male goats of the Saanen x *Naine de Kabylie* crossbred from the same farm and were selected from a larger experiment based on similar body weight (25 ± 0.8 kg), age at slaughter (240 ± 8 days), and all slaughtered on the same day under equivalent slaughtering conditions according to industrial and cultural practices (Lamri et al., 2023). The goats were reared under traditional and extensive production systems in the Kabylia Mountains (North of Algeria). Before slaughter, the animals were transported one day before to the abattoir and kept overnight without feeds but with free access to water. In order to avoid the seasonal effect, the animals were from the batch slaughtered in March. The animals were humanely slaughtered in the same slaughterhouse in the Kabylia region, in compliance with the Halal slaughter method (based on Islamic legislation). In this type of slaughter, the goats were not stunned. The animals were dressed following routine commercial slaughterhouse procedures. After exsanguination, the carcasses were split into two equal halves along the vertebrate column. The carcasses were kept under standard chilling conditions (4 ± 2°C).

2.2. Semitendinosus muscle sampling

Semitendinosus (ST) muscle samples from the distal part were collected from a random side of each goat carcass, at three different time points. The initial samples were taken within 1h post-mortem and the two others from the same cuts and carcasses (fully randomized between the left and right) kept in a chilling room at 4 ± 1 °C were taken at 8h and 24h post-mortem for a total of 24 biopsy samples. An approximate of 10 g for the biochemistry and proteomics analyses were removed, chopped into small pieces using sterile scalpels, snap-frozen in liquid nitrogen and stored at −80°C until the extraction of muscle proteins.

2.3. Profiling and characterization of goat Semitendinosus muscle using shotgun proteomics

2.3.1. Muscle protein extraction and quantification

The 24 individual goat muscle samples stored at -80°C were analyzed the same day and under the same conditions of buffer and extraction protocol to recover the total muscle proteins (*i.e.,* both sarcoplasmic and myofibrillar proteins) following previous procedures (Bouley, Chambon, & Picard, 2004; Gagaoua, Troy, et al., 2021). Briefly, 150 mg of the samples from each individual and post-mortem time (1, 8 and 24h), firstly randomized to double blind for the sampling time, were mixed with 3 mL of fresh buffer containing 2 M thiourea, 1.2% DL-

dithiothreitol, 8 M urea, 1% Pharmalyte 3−10 (GE Healthcare, Uppsala, Sweden) and 2% CHAPS. The samples and protein homogenates were handled during the entire extraction process in wet-ice and incubated at 4°C for 15 min before homogenization using a Polytron homogenizer (model PT2100, Kinematica AG, Littan/Luzern, Switzerland) at 20,000 rpm for 45 seconds. Afterwards, the homogenates were kept once again in wet-ice and shacked for 25 min before centrifugation at 10,000 x *g* at 4°C to remove insoluble proteins, connective tissue, fat and other debris. The supernatant was then collected in Eppendorf tubes and stored at -80°C for further analyses in terms of protein quantification, SDS-PAGE analyses and proteome profiling and characterization.

The quantification of the total proteins, in triplicate, was performed using the Bio-Rad protein assay kit (Bio-Rad Laboratories, Hercules, CA, USA) based on the Bradford method (Bradford, 1976). Serum albumin from bovine (BSA) was used as a standard at a concentration of 1 mg/mL.

2.3.2. Protein bands preparation for shotgun proteomics using one-dimensional SDS-PAGE electrophoresis

To gather all the protein extracts in one tiny band before shotgun proteomics (Y. Zhu et al., 2021), the muscle protein extracts were first denatured by mixing at 1.0:1.0 (v/v) with a standard Laemmli sample buffer 2× concentrate (#S3401, Sigma-Aldrich, St. Louis, USA) containing 125 mM Tris (pH 6.8), 20% v/v glycerol, 4% w/v SDS, 10% v/v β-mercaptoethanol and 0.004% bromophenol blue. Then, the samples were vortexed and incubated at room temperature for 5 min before heating at 90 °C for 10 min using a standard block heater (VWR, International). The denatured proteins (40 μg for a final volume of 20 μL) were subsequently loaded into standard 12% resolving and 4% stacking gels of sodium dodecyl sulfate polyacrylamide gel electrophoresis (SDS-PAGE) using a Mini-PROTEAN Tetra Cell system (Bio-Rad Laboratories, Hercules, CA, USA) at 4 watts during 15 min to concentrate the proteins in one tiny band in the stacking gel. A TGS running buffer (#T7777, Sigma-Aldrich, Saint Louis, USA), containing 25 mM Tris (pH 8.6), 192 mM glycine and 0.1% SDS was used. Afterwards, the gels were washed several times with Milli-Q water, stained with EZ Blue Gel staining reagent (Sigma- Aldrich, Saint Louis, USA) for around 10 min and subjected to several other washes with Milli-Q water under gentle shaking. The protein bands from each animal were excised from the washed gels using sterile and disposable scalpels, immediately placed into sterile Eppendorf tubes to be reduced, alkylated, destained and dried, before liquid chromatography-tandem mass spectrometry (LC-MS/MS) analyses (Gagaoua, Troy, et al., 2021; Picard et al., 2016).

2.3.3. LC-MS/MS analysis, protein identification and preparation of the proteome database

Before LC-MS/MS, the dried protein bands stored at -20 °C were first digested by a sequence grade Trypsin (Promega, USA) following the conditions previously described (Y. Zhu et al., 2021). The samples were analyzed by means of a Dionex UltiMate 3000 system (nanoelectrospray ion source) coupled to a Q Exactive[TM] HF-X hybrid Quadrupole-Orbitrap mass spectrometer (Thermo Fisher Scientific). A C18 column was used to desalt the peptide fractions before LC–MS/MS analysis according to the manufacturer's instructions. The peptides were loaded with C18 PepMap trap column (Thermo Fisher Scientific) and washed with pure water (98%), acetonitrile (ACN, 2%) and formic acid (0.01%) with a flow rate of 10 μl/min. After 6 min, the trap column underwent reversed-phase high-performance liquid chromatography (RP-HPLC) using an EASY nLC self-filling column (Thermo Fisher Scientific, Germany). Mobile phase A of the reversed -phase HPLC consisted of 0.1% formic acid in pure water, and mobile phase B consisted of 95% ACN acetonitrile with 0.1% formic acid. The peptides were separated using a 40-min gradient method at a flow rate of 300 nL/min. The peak identification of the peptides and raw files of LC-MS/MS were screened and aligned against *Capra hircus* (goat) database (UP000291000, 32,609 sequences). The digestive enzyme was set to trypsin to search for the mass spectrometry data in the retrieval database. The maximum missing cleavage sites were set to 2, and the tolerances of precursor ions and fragment ions were 5 ppm and 0.02 Da, respectively. The aminomethylation of cysteine was a fixed modification, and acetylation of the protein N-terminal and lysine and methionine oxidation were variable modifications. The database search results were screened and exported when the false discovery rate (FDR) of the peptide spectrum and protein match level was < 1%.

2.4. Statistical analyses

The screening criteria for both the proteins and peptides were set at > 99 % confidence at an FDR ≤ 1 %. Then, the proteome data were processed after log2-transformation and Pareto-scaling of the data peak intensities using R software. Values with a coefficient of variation < 0.2 and Z-scores centralized and missing values were normally distributed. The missing values were computed using k-nearest neighbors based on similar features (KNN feature-wise) as previously described (Stacklies, Redestig, Scholz, Walther, & Selbig, 2007). The volcano plots were carried out to identify the differentially abundant proteins (DAPs) during the early post-mortem times in the goat *Semitendinosus* muscle proteome using three pairwise comparisons: 1h *versus* 8h, 8h *versus* 24h, and 1h *versus* 24h. For each comparison, the volcano plots were constructed to

analyze the DAPs having fold change of 1.5 and *P* <0.05 with a Benjamini−Hochberg FDR correction set at *P* <0.01. The common changing proteins within the three comparisons were further projected in a Principal Component Analysis (PCA) to investigate their suitability to discriminate the three post-mortem times (Gagaoua, Bonnet, De Koning, & Picard, 2018). The software XLSTAT 2021 1.2.2. (Addinsoft SARL, París, France) was used for PCA analysis based on Z-scores. Furthermore, Sparse Partial Least Squares-Discriminant Analysis (sPLS-DA) was run using the full proteome database to identify putative biomarkers of ageing allowing the classification and discrimination of the three post-mortem times (Lê Cao, Boitard, & Besse, 2011). Variable importance in projection (VIP) was calculated and the top 20 proteins allowing the separation in the sPLS-DA model are retained and compared to the list of DAPs.

2.5. Bioinformatics analyses

For bioinformatics, several analyses were performed (Kiyimba, Gagaoua, Suman, Mafi, & Ramanathan, 2022). First, the protein-protein interactions (PPI) between the DAPs proteins for each of the three conditions were analyzed using STRING database v11.0 (https://string-db.org/) to build protein networks. The confidence interval and FDR stringency were receptively set at 0.5 and 1.0 (high percent), in order to obtain as many representative significant features and interactions. For each PPI, the DAPs were categorized into eight molecular functions using manual annotation as previously described (Gagaoua, Warner, et al., 2021). Second, the enrichment analysis of the pathways was investigated using Metascape®, an open-source tool (https://metascape.org/). Thus the enriched Gene Ontology (GO) terms were investigated for the three DAPs proteins lists or all the changing proteins taken together. We further investigated the overlap and functional connections among the three DAPs protein lists based on a Circos plot and comparison of the enriched GO terms among the 3 different time comparisons by means of hierarchical heatmap clustering. A network based on GO enriched terms has been generated with a cut-off criterion set at a minimum count of 3 gene entries, an enrichment factor > 1.5, and a P-value < 0.01. Hierarchical heatmap clustering was constructed using the DAPs between 1 and 24h post-mortem within the up- and down-regulated proteins at 1h post-mortem.

3. Results

The shotgun proteomics allowed quantifying 748 proteins at an FDR of 1%, a minimum of 3 count peptides for each protein and less than 3% missing data as filtering criteria in the goat *Semitendinosus* muscle proteome in the 24 samples. The statistical comparisons identified a total of 174 proteins as differentially abundant across the three post-mortem times (1, 8 and 24 h);

detailed information on the DAPs are depicted in **Table 1**. The DAPs were found, after manual annotation using several databases, to belong to 8 main molecular functions (**Table 1**), these being i) Binding, transport and calcium (Ca^{2+}) homeostasis (n = 58); ii) Catalytic, metabolism & ATP metabolic process (n = 30); iii) Muscle contraction, structure and associated proteins (n = 29); iv) Oxidative stress, response to hypoxia & cell redox homeostasis (n = 15); v) Ribosomal proteins (n = 10); vi) Proteolysis & associated proteins (n = 9); vii) Chaperones and/or heat shock proteins (n = 9) and a group of viii) Miscellaneous proteins (n =14), which grouped features playing other functions.

The pairwise comparisons by means of Volcano plots analyses allowed within the three comparisons to identify 55, 52 and 154 DAPs, for 1h-8h, 8h-24h, and 1h-24h, respectively (**Table 1**). The fold change (FC), log2 of FC and p-values of these DAPs are depicted in **Table 1**. Twelve proteins (gene names) were found to be changing whatever the post-mortem time (comparison), and they are shown in bold characters in **Table 1**. The percentages of the distribution of the 174 DAPs proteins within the eight functional pathways across the three comparisons are given in **Table 2**. Interestingly and whatever the comparison, the number of proteins from binding, transport and calcium homeostasis pathway is equivalent among all the comparisons (ranging from 33 to 35%), whereas catalytic, metabolism & ATP metabolic process pathway was more important early post-mortem for 1h-8h (24%) than the others, hence depicting the importance of energy metabolism in the conversion of muscle into meat very early post-mortem. Similarly, proteolysis & associated proteins were more significant very early post-mortem than any other comparison. Inversely, the number of proteins belonging to oxidative stress, response to hypoxia & cell redox homeostasis as well as chaperones and/or heat shock protein pathways were less involved between 1h-8h (4%) compared to 8h-24h (10-11%). In the following sections, detailed results for each comparison are given.

3.1. Comparison of the goat Semitendinosus muscle proteome between 1h and 8h post-mortem

From the 55 DAPs identified in the goat *Semitendinosus* muscle proteome to differ between 1h and 8h post-mortem (**Table 1**), 5 were up-regulated (PMSD4, HSDL2, CASQ2, STRAP, and MYOZ3) and 50 were down-regulated at 1h post-mortem (**Fig. 1A**). The pathway enrichment analysis of this protein list revealed 15 significantly enriched terms (**Fig. 1B**). The statistics details of each GO term are given in **Table S1** and the association between the enriched terms and their functional enrichment are further reported by the functional GO network of **Fig. S1**. Among these, the top 8 enriched terms were energy derivation by oxidation of organic

compounds (GO:0015980), heart contraction (GO:0060047), actomyosin structure organization (GO:0031032), proteolysis involved in protein catabolic process (GO:0051603), cellular carbohydrate catabolic process (GO:0044275), NADH metabolic process (GO:0006734), proton transmembrane transport (GO:1902600) and mitochondrial transmembrane transport (GO:1990542). The PPI network of the 55 DAPs is given in **Fig. 1C**. The network revealed interconnectedness among the functional pathways, mainly among the four major pathways, these being binding, transport and calcium homeostasis, catalytic, metabolism & ATP metabolic process, muscle contraction, structure and associated proteins and proteolysis & associated proteins. Only four proteins (SPR, GSTM3, SGTA and NDRG2) showed no interactions, but the large majority of proteins were all inter-related allowing the creation of a unique interacting network.

3.2. Comparison of the goat Semitendinosus muscle proteome between 8h and 24h post-mortem

As shown in **Table 1**, 52 DAPs were different in the goat *Semitendinosus* muscle proteomes at 8h and 24h post-mortem. The results of the volcano plot evidenced 10 proteins (NAPG, DYNC1H1, CAMK2D, NAP1L4, P4HB, MYH13, MYOM3, PGP, CFH, and EIF5A) to be up-regulated in the goat *Semitendinosus* muscle at 8h post-mortem, whereas, 42 were down-regulated (**Fig. 2A**). The pathway enrichment analysis revealed 13 significantly enriched GO terms (**Fig. 2B**). The statistics details of each GO term are given in **Table S2** and the association between the enriched terms and their functional enrichment are further reported by the functional GO network of **Fig. S2**. Among these, the top 5 enriched terms were peptide metabolic process (GO:0006518), glycerol metabolic process (GO:0006071), muscle system process (GO:0003012), sulfur compound metabolic process (GO:0006790), small molecule catabolic process (GO:0044282) and cellular macromolecule catabolic process (GO:0044265). The PPI network of the 52 DAPs is given in **Fig. 2C**, evidencing a network of 40 edges with 18 proteins that were not interconnected. The PPI network revealed also an interconnectedness among the different functional pathways we identified in this study.

3.3. Comparison of the goat Semitendinosus muscle proteome between 1h and 24h post-mortem

As expected, a very high number of proteins (154 DAPs) are changing between 1h and 24h post-mortem (**Table 1**), from which 127 proteins were down-regulated and 27 up-regulated at 1h post-mortem (**Fig. 3A**). This highlight major dynamic changes occurring in the post-mortem

Semitendinosus muscle. The 27 up-regulated DAPs at 1h than 24h post-mortem are involved in muscle contraction (n = 8; MYOM3, CASQ2, SPTB, FLNC, SNTB1, MYH14, TPM3, FKBP3), binding, transport and calcium homeostasis (n = 8; CAMK2D, SYNPO2, FABP5, JSRP1, CAV1, DBI, ATP2A2, TKT) and proteolysis and associated proteins (SERPINA3 and PSMA3). The pathway enrichment analysis performed on the 154 proteins revealed 20 significantly enriched terms (**Fig. 3B**). The statistics details of each GO term are given in **Table S3** and the association between the enriched terms and their functional enrichment are further reported by the functional GO network of **Fig. S3**. The top 3 enriched GO terms clusters were muscle system process (GO: 0003012), generation of precursor metabolites and energy (GO:0006091) and peptide metabolic process (GO:0006518). These were followed mainly by muscle structure development (GO:0003012), actomyosin structure organization (GO:0031032), small molecule catabolic process (GO: 0044282), multicellular organismal movement (GO:0050879), sulfur compound metabolic process (GO:0006790), and cellular ketone metabolic process (GO:0042180). The PPI network revealed a strong interconnectedness between the proteins and the functional pathways to which they belong (**Fig. 3C**). To the best of our knowledge, this is the first comprehensive PPI network depicting the dynamic changes occurring in early post-mortem muscle revealed by shotgun proteomics. Such complexity of the mechanisms is further confirmed by the hierarchical heatmap clustering of the 154 up- and down-regulated proteins between 1h and 24h post-mortem (**Fig. 4**). The findings highlighted among other enriched terms, that regulation of proteolysis (GO:0030162), muscle structure development (GO:0061061) and muscle system process (GO:0003012) are common changing pathways. Interestingly, one GO term was exclusively enriched at 1h post-mortem only, this being vascular process in circulatory system (GO:0003018), while 40 GO terms were significantly enriched at 24h post-mortem only (**Fig. 4**).

3.4. Protein overlap and comparison of the DAPs changing during the post-mortem period

Functional enrichment analysis and clustering on the total DAPs identified to change in the goat *Semitendinosus* muscle proteome among all post-mortem time comparisons are given in **Fig. 5**. The overlap among the three protein lists revealed 12 common proteins: SLC25A3, SIRT2, FHOD1, PDCD6IP, GPD2, SPR, UCHL3, RPS3A, SGTA, MYOZ2, GSTM3 and NDRG2 (**Table 1**, **Fig. 5A** and **Fig. S4**). These proteins belong to five 5 significantly enriched GO terms (**Fig. 5B**) mainly dominated by proteolysis involved in the protein catabolic process (GO:0051603). The abundances of these common proteins were increasing during the post-mortem time (**Fig. 5C**), and their projection in a PCA analysis allowed a clear separation of the three post-mortem times (**Fig. 5D**).

The hierarchical heatmap clustering of the total DAPs of each condition (1h-8h, 8h-24h and 1h-24h) revealed 6 common enriched terms (**Fig. 5E**), these being carbohydrate metabolic process (GO:0005975), proteasome-mediated ubiquitin-dependent protein catabolic process (GO:0043161), actomyosin structure organization (GO:0031032), positive regulation of organelle organization (GO:0010638), muscle system process (GO:0003012) and generation of precursor metabolites and energy (GO:0006091). The dominant GO terms are further shown in a functional network (**Fig. 6A**), depicting the degree of interconnectedness of the dynamic changes occurring early post-mortem in the goat muscle. Among these GO terms, those related to the muscle system process, generation of precursor metabolites and energy, actomyosin structure organization and carbohydrate metabolic process were more abundant in the 1h-24h comparison. Furthermore, it must be noted that the tricarboxylic acid cycle (GO:0006099), mitochondrial calcium ion homeostasis (GO:0051560), positive regulation of apoptotic process (GO: 0043065), autophagy (GO:0006914) and cellular ketone metabolic process (GO:0042180) were significantly and exclusively specific to the goat *Semitendinosus* muscle proteome comparison between 1h and 24h post-mortem, whereas, glycerol metabolic process (GO:0006071) was for the comparison between 8h-24h post-mortem. The full functional enrichment of the top 20 GO clusters with their representative enriched terms (one per cluster) are given in **Fig. 6B**.

3.5. Discrimination of post-mortem times by means of chemometrics

The sparse partial least-squares discriminant analysis (sPLS-DA) allowed a clear separation of the three post-mortem times (**Fig. 7A**). Several proteins allowed achieving a clear separation based on their VIP scores, depicting in **Fig. 7B** the most contributing 20 proteins. Our findings corroborate those of an earlier study that used two-dimensional electrophoresis and chemometrics for the profiling of post-mortem changes at different sampling times in bovine muscle (X. Jia, Hildrum, et al., 2006). The authors revealed 39 changing proteins originating from 47 spots, allowing a clear separation of the post-mortem times. In this study, only NAP1L4 showed a higher content in the goat *Semitendinosus* muscle at 1h post-mortem, whereas 19 proteins were abundant at 24h post-mortem, and intermediate for 8h post-mortem. Interestingly, 11 proteins out of the 12 common proteins (PDCD6IP, FHOD1, SGTA, GSTM3, MYOZ2, SLC25A3, SIRT2, NDRG2, GPD2, SPR and RPS3A) belong to the list of the top 20 proteins. They can be proposed as candidate biomarkers of post-mortem ageing (storage time) and goat meat quality.

4. Discussion

With the growing world's population and demand for animal proteins, goat meat represents an alternative and sustainable meat source of high-quality (a lean meat with relatively low-fat content and cholesterol intake), making it a potential competitor to conventional red meat sources (Lamri et al., 2022; Mazhangara, Chivandi, Mupangwa, & Muchenje, 2019). However, there is a need to strengthen our knowledge on the factors underpinning the biochemical mechanisms at interplay in goat meat quality determination. As stated, meat is a consequence of myriad mechanisms taking place in muscle since the first hours following animal bleeding and continue during the post-mortem and ageing periods (Gagaoua, Duffy, et al., 2022). Recently, the application of proteomics in meat research has yielded valuable insights over conventional methods (Purslow et al., 2021), hence contributing greatly to a better understanding of the complexity of the muscle proteome and its importance in determining meat quality (Gagaoua, Schilling, et al., 2022). Despite this, to date and to the best of our knowledge, the dynamic changes in goat muscle proteome have never been studied, and the existing few recent label-free proteomics studies are limited to the comparison of goat breeds or to the impact of freezing storage on meat properties (Di Luca et al., 2022; Gu, Wei, Zhang, & Liu, 2020; W. Jia et al., 2021). Therefore, shotgun proteomics, coupled with bioinformatics and chemometrics, were applied in this study to investigate the modifications in the protein abundances occurring early post-mortem in *Semitendinosus* muscle proteome of goats, with the aim of deciphering the molecular signatures at interplay. We further attempt to discover putative protein biomarkers that can be used to monitor the early post-mortem phase of muscle into meat conversion, and consequently develop strategies ensuring high-quality goat meat products. This can be performed based on reference values for each biomarker; monitoring the production process to ensure that the meat products meet the established reference values; adjustments to the production process can be made to ensure that the biomarker levels are optimized for high-quality meat products; and finally quality control measures can be implemented to ensure that the meat products meet the desired quality standards.

In this study, the temporal proteomics profiling of the *Semitendinosus* post-mortem muscle evidenced substantial dynamic changes along with the involvement of myriad and interconnected biological pathways, some of which were never revealed before, even in beef or pork muscles. Thanks to the proteomics protocol we applied, a thorough profiling of the observed changes was made possible. Proteins involved in binding, transport and calcium homeostasis and others from the muscle contraction and structure exhibited an equivalent contribution during post-mortem storage, demonstrating the central role in driving the processes taking place in post-mortem muscle (England, Scheffler, Kasten, Matarneh, & Gerrard, 2013; Gagaoua, Troy, et al., 2021;

Lana & Zolla, 2016; Ouali et al., 2013). Catalytic, metabolism and ATP metabolic process, and proteolysis were found active pathways since the first hours following animal bleeding. Conversely, oxidative stress, response to hypoxia and cell redox homeostasis along chaperones and heat shock proteins as key players of stress response accounted for the large proportion of the biochemical processes taking place more significantly after 8h post-mortem. These suggest that oxidative processes occur at weak or moderate intensity around 1h post-mortem. This study is the first to reveal these important molecular signatures including the rate at which they evolve. The generation and accumulation of reactive oxygen species (ROS) early post-mortem due to the intense catalytic activity of the energy metabolism pathways, especially from mitochondria, activate the endogenous antioxidant defense systems of muscle (W. Zhang, Xiao, & Ahn, 2013). Studies described that an increase in the ROS content in post-mortem muscle cells might affect the biochemical metabolism, apoptosis onset and thereby meat tenderization (Gagaoua, Terlouw, et al., 2021; Lana & Zolla, 2015; Malheiros et al., 2019). Apoptosis has been reported to initiate immediately after slaughter (Laville et al., 2009). The down regulation of anti-apoptotic factors enhances the cell death process, which consequently increases meat tenderization through the proteolysis of myofibrils by activated caspases among other proteases (Gagaoua, Hafid, et al., 2015; Ouali et al., 2013; V. Sierra & Olivan, 2013). Together with the anoxic and oxidative stress caused by the acute loss of oxygen, skeletal muscle cells are more likely to enter apoptosis through the intrinsic pathway rapidly after exsanguination (Rønning, Andersen, Pedersen, & Hollung, 2017). Concerning autophagy, it is thought to function as a survival process in delaying apoptosis onset (Lum et al., 2005).

The GO enrichment analyses further evidenced the central role of energy derivation by oxidation of organic compound and peptide metabolic process pathways, followed by others related to mitochondrial transport, calcium homeostasis and regulation of apoptosis. Our findings confirmed that the conversion of muscle into meat is largely orchestrated by energy production as well as mitochondrial metabolism and homeostasis through calcium and permeability transition regulation. It is therefore not inconceivable to speculate that mitochondria as key players in the generation and regulation of cellular bioenergetics, are central to myriad events contributing to the development of meat quality (Dang et al., 2020; Gagaoua, Warner, et al., 2021; Ouali et al., 2013; Purslow et al., 2021; V. Sierra & Olivan, 2013).

Interestingly, the hierarchical heatmap (**Fig. 4**) revealed that the significant enrichment of "regulation of proteolysis", "muscle structure development" and "muscle system process" are common features, confirming the hypothesis that proteins of structure and contraction are

degraded as early as the first few hours after death, albeit in different proportions and rates (Lana & Zolla, 2016). The "vascular process in circulatory system" was the only term specifically enriched in the proteome at 1h post-mortem, which makes sense and is consistent with residual blood flow in the first minutes or hours after the bleeding of the animal (Ouali et al., 2013). In the following sections, we discuss in-depth the functions and metabolic pathways to which certain of the differentially abundant proteins belong, some of which may be proposed as candidate biomarkers to monitor the dynamic changes in goat *Semitendinosus* muscle during the postmortem period and its final meat quality.

4.1. Pivotal role of binding, transport and calcium homeostasis pathway

The binding, transport, and calcium homeostasis pathway has been identified as the major signature characterizing the early post-mortem modifications in goat *Semitendinosus* muscle. Overall, most of the DAPs proteins belonging to this pathway were down-regulated at 1h post-mortem. Among the few up-regulated proteins, CASQ2 (calsequestrin-2) and STRAP (Serine-threonine kinase receptor-associated protein) were more abundant at 1h compared with 8h. CASQ2 is one of the most abundant calcium-binding proteins localized in the sarcoplasmic reticulum lumen, which stores calcium and modulates its homeostasis until it is needed for muscle contraction (Picard et al., 2016; Rossi et al., 2022). Calcium release and sequestration are critical mechanisms to regulate muscle contraction and relaxation (Purslow et al., 2021). Therefore, its primary role is to maintain a high amount of calcium in the sarcoplasmic reticulum (Guo et al., 2016). The pivotal role of calcium in post-mortem muscle and meat tenderization is well-known, mainly in the regulation of proteolytic enzymes and cellular metabolism (Ouali et al., 2013) and beyond that, for muscle function and plasticity (Berchtold, Brinkmeier, & Müntener, 2000). Thus, it is reasonable to propose that disruption of the sarcoplasmic reticulum membrane would increase the abundance of calcium-binding proteins since the early post-mortem. Indeed, calcium is the main regulatory and signaling molecule of skeletal muscles, therefore, its monitoring is central to understand the rate and extent of post-mortem processes (Purslow et al., 2021). Mitochondria, a pluripotent organelle identified in this study to play a central role, is also involved in calcium homeostasis, apoptosis and post-mortem muscle changes (Contreras, Drago, Zampese, & Pozzan, 2010; Hudson, 2012; Ouali et al., 2013). In fact, calcium overload induces intercellular stress that might damage the integrity of mitochondria, more importantly in the first hour following animal death, hence releasing cytochrome c and pro-apoptotic factors, thereby triggering the intrinsic apoptotic pathway with the consequences it might have on muscle structure degradation (England et al., 2013; Gagaoua, Terlouw, et al.,

2021; Lana & Zolla, 2015, 2016; Ouali et al., 2013). Other proteins involved in calcium homeostasis were further identified as more abundant at 1h post-mortem compared with 24h, namely CAMK2D, CAV1, and ATP2A2 (**Table 1**), all of which regulate calcium influx/release in skeletal muscles. In the context of meat quality, several proteins of this pathway were previously identified as biomarkers of different quality traits of beef (Gagaoua, Terlouw, et al., 2021; Picard & Gagaoua, 2020), lamb (Cheng et al., 2020) and pork (Hou et al., 2020), thus demonstrating their importance in meat quality determination. The higher abundance of STRAP at 1h post-mortem further supports the important role of Serine/threonine kinases in the apoptotic processes (Cross et al., 2000).

From the down-regulated proteins at 1h post-mortem several are responsible for transmembrane phosphate transport (SLC25A12, TIMM44, COQ9, SLC25A12) or calcium binding (ATP1B1, ATP2A1, ATP2A2), which are pivotal in controlling the exchange of ADP/ATP across the membrane, mitochondrial permeability transition pore or cytosolic calcium ions concentration (Kwong et al., 2014). In response to apoptotic stimuli, several pro-apoptotic factors cause mitochondrial outer membrane permeability (MOMP) and form pores such as Bax/Bak, in the outer membrane, which allows the release of cytochrome c from its binding sites (Peña-Blanco & García-Sáez, 2018; Tait & Green, 2010). Once MOMP has been achieved, the apoptotic response is irreversibly triggered. Thus, the formation of mitochondria permeability transition pore on the membrane is the key step of this pathway, and the regulation is focused on the steps leading to MOMP, which can be suppressed or promoted by inhibitor or promoter molecules, respectively. In meat research, these pathways including the implication of membrane permeability transition pore in meat tenderization, for instance in beef and pork, has been investigated (Dang et al., 2020; Dang et al., 2022; L.-L. Wang, Han, Ma, Yu, & Zhao, 2017; J. Zhang, Ma, & Kim, 2020).

As carrier proteins, the greater abundance of the proteins from programmed cell death pathway just after the first hour post-mortem may indicate a greater mitochondrial activity, in line with previous research, for instance in bovine muscle (Yu et al., 2018; Zhai et al., 2020). Several of the DAPs proteins such as PDCD6IP (programmed cell death 6 interacting protein) are also directly involved in apoptosis (Y. Wang, Jin, Xia, & Chen, 2022), and found in this study to increase in abundance over time. Currently, this is the first time that PDCD6IP is identified in the post-mortem muscle proteome as related to meat tenderization. Refers to meat quality, a transcriptomic study on cattle identified PDCD6IP as a potential transcript target of variation in beef tenderness (Gonçalves et al., 2018). FHOD1 (FH1/FH2 domain-containing protein 1) is

another common protein (**Figure 5**), which is an important regulator of muscle cell biology and myofibrillar maintenance (Schönichen et al., 2013). FHOD1 was previously identified in one proteomics study to be related with beef texture (Yao Zhu et al., 2021), thus proposing it as a hallmark of the cytoskeleton integrity. Finally, SIRT2 (sirtuin 2), a NAD-dependent deacetylase that primarily functions in the cytoplasm and regulates α-tubulin acetylation levels, is in this study another common protein that increases in abundance over time. SIRT2 is part of the Sirtuins family of proteins involved in the regulation of mitochondrial activity (Lombard, Tishkoff, & Bao, 2011), metabolic adaptation including glucose metabolism (Lee, Lee, Park, & Jeong, 2022) and autophagy (Han et al., 2021). Despite these different roles, nothing is yet known about Sirtuins in post-mortem skeletal muscle and meat research. The down-regulation of SIRT2 at 1h and 8h post-mortem might evidence a less activity in membrane trafficking events. However, the knowledge available in the literature is limited to human diseases, for this reason, the role of SIRT2 in maintaining cellular homeostasis during the post-mortem period should be profoundly investigated.

4.2. Pivotal role of catalytic, metabolism & ATP metabolic process

The identification of a high number of DAPs from the energy metabolism pathway early post-mortem phase agrees with the growing body of knowledge supported by previous studies (Bjarnadottir, Hollung, Faergestad, & Veiseth-Kent, 2010; Gagaoua et al., 2020; X. Jia et al., 2007; Ouali et al., 2013). Indeed, earlier proteome experiments focusing on modifications in post-mortem muscle have found that ATP is available in muscle cells through the first 24 h after animal death, mainly when part of the energy generation is still operative (X. Jia et al., 2007). Among the 13 DAPs identified to differ between 1h and 8h post-mortem, HSDL2 (hydroxysteroid dehydrogenase-like protein 2), a member of the short-chain dehydrogenases/reductases superfamily located in the mitochondria, was the only over-abundant protein at 1h post-mortem. It has been reported that lipids, the essential regulators of cellular stabilization and metabolism, have proven to be involved in post-mortem energy production (Ouali et al., 2013). It is worth mentioning that the role of lipids is highly mediated by their binding proteins, in support of the high number of binding and transport proteins identified in this trial (**Table 1** and **Figure 3**). Higher abundance of lipid metabolism pathways in muscle proteome during the early post-mortem period was previously evidenced by proteomics (Yu et al., 2018; Zhai et al., 2020). HSDL2 was also recently identified abundant in beef tenderloin muscle with lower tenderness (Li & Li, 2021). The greater abundance observed at 1h post-mortem in the goat muscle confirms this statement. Further comparisons of the proteins changing

between 1h and 24h revealed a greater abundance at 1h post-mortem of GYS (glycogen [starch] synthase), an enzyme that regulates glycogen synthesis, and GOT2 (aspartate aminotransferase, mitochondrial) which plays a key role in amino acid metabolism. The greater abundance of GOT2 has been previously associated with higher oxaloacetate production and color stability in beef *Longissimus thoracis* muscle proteome (Ramanathan et al., 2021). Additionally, GOT2 has been suggested as a potential biomarker of dark-cutting beef defect (Gagaoua, Warner, et al., 2021), although contrasting results have been reported (Sentandreu et al., 2021).

Several proteins belonging to complex I, II, III, and IV, which were involved in the mitochondrial electron transport chain (UQCRB, COX4I1, NDUFV1, NDUFA4, NDUFB8, NDUFS2, ATP5PD, and AGL) and tricarboxylic acid cycle (ACO1, FH and IDH3B) were found to be down-regulated in goat proteome at 1h compared to 8h and 24h post-mortem. Usually, the greater abundance of mitochondria electron transport proteins, due to their relationship to the increase of calcium concentration (Wu et al., 2020; Yang et al., 2018), is associated with greater proteases activity and post-mortem proteolytic processes (Gagaoua, Terlouw, et al., 2021; Ouali et al., 2013). In the context of early post-mortem time, different proteins involved in the oxidative phosphorylation system (OXPHOS) were recently identified in beef as less abundant after 6 hours post-mortem (Ding, Wei, Liu, Zhang, & Huang, 2022). Refers to goat muscle proteome, proteins related to the electron transport chain were previously identified as related to meat quality (Wei, Li, Zhang, & Liu, 2019) or frozen meat quality (W. Jia et al., 2021), while, to the best of our knowledge, this is the first time that is related to early post-mortem processes. However, the up-regulation, over post-mortem time, would reflect the mechanism of maintaining homeostasis or struggle to survive in muscle cells (Ji, Liu, & Luo, 2022).

Taken all together, the goat muscle proteome changes during the early post-mortem is accompanied with a shift in post-mortem muscle energy metabolism towards several energy pathways whether they are from the glycolytic or aerobic oxidative energy yielding phases. These findings are in line with the recognized knowledge on the role that play metabolites, enzymes, and enzyme activity in post-mortem muscle metabolism, and their impact on ultimate meat quality (England et al., 2013; Matarneh et al., 2023; Wicks et al., 2022). Finally, the changing enzymes in this trial might be explained by the aim of replenishing the ATP levels in the muscle in an attempt of maintaining muscle in a relaxed state (X. Jia, Hildrum, et al., 2006).

4.3. Muscle contraction, structure and associated proteins including extracellular matrix

During post-mortem time, apoptosis can affect skeletal muscle integrity through the modulation of calcium flow with implications on muscle ultrastructural changes, hence playing a pivotal role in the determination of final meat quality (Gagaoua, Terlouw, et al., 2021; Gagaoua, Troy, et al., 2021; Warner et al., 2021). The disruption of sarcoplasmic reticulum might increase sarcoplasmic calcium concentrations, activating the endogenous proteases such as calpains and caspases to promote proteolysis. The hydrolysis of the muscle membranes by these proteases significantly damages the integrity of the cytoskeleton and permeability of the cell membrane, which is involved in meat tenderization. Among the differentially abundant proteins, MYOZ3, an actinin and gamma-filamin binding was the only protein abundant at 1h post-mortem. MYOZ3 is mainly expressed in fast-twitch muscle fibers, that participate in the calcium-mediated signal pathways thereby regulating muscle fiber differentiation and meat tenderness determination (Yao Zhu et al., 2021). Generally, members of the myozenin family, due to their ability to interact with troponin and myotilin in the skeletal muscle Z-disks, are associated with the disorganization of sarcomere during the post-mortem period (D'Alessandro & Zolla, 2013) and members were proposed as biomarkers of beef tenderness (Gagaoua, Terlouw, et al., 2021).

Structural proteins composing the thick (MYBPH, MYH6 and MYH7B) and thin filaments (ACTC1, TNNC1, TNNI1, TNNI2, TPM3, TUBA8 and VCL) of sarcomere were found to be less abundant at 1h post-mortem in accordance with the large number of studies proposing them as sensitive targets to monitor the complex biochemical processes taking place during the post-mortem phase (Gagaoua, Terlouw, et al., 2021; Gagaoua, Troy, et al., 2021; Hopkins & Geesink, 2009; Hughes et al., 2014; Lana & Zolla, 2016). It is well known that myosin-binding proteins may play a modulatory role in the regulation of actin-myosin interaction, thus affecting calcium sensitivity (Taylor et al., 1995); consequently, their variation in abundance can reflect apoptosis onset (Gagaoua, Troy, et al., 2021). Among the proteins and in agreement with our findings, a study on beef reported a lower MYBPH abundance at 45 min post-mortem in *Longissimus thoracis* muscle of young bulls as related to both earlier fragmentation and faster early post-mortem metabolism (Gagaoua, Terlouw, Micol, et al., 2015). TNNC1, a calcium-binding subunit of the myofibril thin filament, plays a fundamental role in regulating the excitation-contraction of striated skeletal muscle (Hopkins & Geesink, 2009; Hopkins & Thompson, 2001). In this study, lower amounts of TNNC1 at 1h post-mortem is in agreement with recent proteomics studies (Ding et al., 2022), which reported down-regulation in bovine muscle just after slaughter compared to 24 h, thus confirming its involvement in the ageing process. Refers to goat muscle proteome and/or phosphoproteome studies, several of the above myosins and regulatory proteins

were identified as changing proteins with associations with meat quality (Gu et al., 2020; Wei et al., 2019).

The extracellular matrix proteins (ECM) of skeletal muscles also known as the matrisome, is a complex meshwork consisting of collagens, glycoproteins, proteoglycans, and elastin (Halper & Kjaer, 2014). Two proteins (LAMB1 and LAMC1), belonging to the glycoproteins family of laminins, were down-regulated at 1h post-mortem. Laminins are non-collagen components ensuring the connection of costameres and integrins, which are sarcolemmal membrane-bound protein structures aligned in register with the Z-disks of myofibrils (Csapo, Gumpenberger, & Wessner, 2020). Based on this statement, the less abundance of laminins found at 1h in goat muscle could demonstrate a lower release of ECM glycoproteins, thus confirming that the biochemical processes that affect the degradation of skeletal muscle occur after 24h post-mortem. However, at present, this is the first study that evidenced the involvement of matrisome proteins in the muscle-to-meat conversion period, for this reason, further research are needed using appropriate methods to clarify their role in goat meat quality determination.

4.4. Response to stress: interplay of protein folding and oxidative stress

Exsanguination that occurs in the first hours after slaughter causes oxidative damage to post-mortem muscle cells and leads to subsequent antioxidant response, such as autophagy (Lum et al., 2005). Furthermore, the oxidative stress caused lipid and protein damages are found to account for the occurrence of autophagy in the post-mortem muscle, which afterward affects the post-mortem metabolism and meat quality (Gagaoua, Monteils, & Picard, 2018; Lana & Zolla, 2015; V. Sierra & Olivan, 2013). In this study and among the up-regulated cellular defense and stress proteins at 1h post-mortem, GLO1 (lactoylglutathione lyase) was previously identified in cattle muscle (Yu et al., 2018), although no significant differences were observed throughout the post-mortem times (1, 12, and 24 h). GLO1 is an enzyme that participates in the process of anti-apoptosis. In this study, the higher abundance at 1h post-mortem in goat *Semitendinosus* muscle, indicates that greater enzyme activity and consequently more protection for muscle cells occurred. Most important in this study and in coherence with the important role of apoptosis in the post-mortem processes, a lower abundance of antioxidant proteins (GSTP1, PRDX6, TXN, and PARK7) and heat shock proteins (HSPB1, HSPE1, and HSPB7) was found in the goat proteome at 1h suggesting that oxidative stress and response to stress through molecular chaperones may be involved at moderate intensity in the first hours' post-mortem. In accordance with our findings, GSTP1, a reductant tripeptide involved in cellular detoxification and resistance

to oxidative stress, was identified as over-abundant during meat storage (J. Zhang et al., 2020; W. Zhang et al., 2013).

Among the peroxiredoxin members, PRDX6 is an antioxidant enzyme able to repair membrane damage caused by oxidative stress and prevent cells from apoptosis and autophagy cell-deaths by scavenging ROS (Fisher, 2017). In accordance with our findings, earlier proteomics studies in cattle muscle reported an increase from 10 to 24 h in the abundance of different peroxiredoxin members during the early post-mortem period (X. Jia et al., 2007). The greater abundance of PRDX6 was usually associated with muscle undergoing less oxidative stress, either in the living animals or the muscle post-mortem (Gagaoua, Terlouw, et al., 2021). In the context of goat muscle proteome, PRDX6 was found less abundant early post-mortem in Hengshan goat meat that has greater redness indicating delayed oxidation processes related to meat discoloration (W. Jia et al., 2021). Recently, in the integromics meta-analyses studies conducted by Gagaoua and co-workers, several peroxiredoxins including PRDX6 were found as robust biomarkers of beef tenderness and color (Gagaoua et al., 2020; Gagaoua, Terlouw, et al., 2021). In support of the above, PARK7 (parkinson disease protein 7), known also as DJ-1, is another antioxidant chaperone that plays determinant roles in preventing protein aggregation and denaturation (Rønning et al., 2017). It was here down-regulated at 1h compared with 24h, confirming that oxidative processes may occur later.

Finally, recent proteomics research has associated a series of heat shock proteins (HSPs) with meat quality attributes (Gagaoua et al., 2020; Gagaoua, Terlouw, et al., 2021; Lomiwes, Farouk, Frost, Dobbie, & Young, 2013). HSPs play a determinant role in stress resistance by restoring proteins altered by external stimulus thus assuming a fundamental role in controlling the onset of apoptosis and post-mortem proteolytic processes (Lomiwes et al., 2013; Ouali et al., 2013; Picard & Gagaoua, 2020; Purslow et al., 2021). Studies on goat reported less abundance of small heat shock proteins, like HSPB1 and HSPB7, indicating greater apoptotic status in post-mortem skeletal muscle (Liu et al., 2018; Z. Wang et al., 2016). Our evidence in goat muscle proteome during the early post-mortem time, support previous findings and confirm that HSPs could be effective candidate biomarkers to monitor the morphological and physiological mitochondrial function and regulation of apoptosis.

4.5. Proteolysis and first insights on the involvement of ribosomal proteins

Among the serine protease inhibitors from the serpins superfamily grouped in this study in the proteolysis pathway, only SERPINA3 was previously identified as a target for apoptosis

regulation in post-mortem muscle (Gagaoua, Hafid, et al., 2015; Y. Zhu et al., 2021), while, the explicit relationship of SERPINB1, SERPINF1 and muscle-to-meat conversion processes have not been reported yet. In this study, SERPINA3 was more abundant at 1h post-mortem, whereas SERPINB1 and SERPINF1 were down-regulated. The former is known to play an anti-inflammatory role and is associated to stress (Gettins, 2002). In goat muscle, further studies are needed to better understand the role of serpins in muscle to meat conversion, including in the apoptotic processes. Very few studies reported serpins in the muscle proteome of small ruminants (della Malva et al., 2023; Zhao et al., 2022), and our study is the first time to relate them to the biochemical processes taking place in the early post-mortem time of goat muscle. Therefore, our evidence highlights that there is a need to elucidate the dynamic changes of this important superfamily of proteins in meat tenderization.

Several members of the ubiquitin–proteasome pathway were further found to be involved in the conversion of goat post-mortem muscle into meat (**Table 1**: PSMA3, PSMA4, PSMD3, PSMD4, PSMD5 and UCHL3), with a specific enriched GO term "proteasome-mediated ubiquitin-dependent protein catabolic process" whatever the post-mortem time (**Figure 6**). More importantly, the central GO network evidenced interaction of this GO term with both "autophagy" and "positive regulation of apoptotic process", supporting the pivotal role of proteolysis in the post-mortem degradation of muscle proteins, response to oxidative stress and cell death (Shang & Taylor, 2011). The proteasome is a multicatalytic proteinase complex that can degrade proteins in the cytosol and nucleus, with the 20S multicatalytic structure of the 26S proteasomes having an efficient proteolytic activity (Goll, Neti, Mares, & Thompson, 2008), evidenced by earlier studies on myofibrillar structures such as myosin, nebulin, actin and tropomyosin (Robert, Briand, Taylor, & Briand, 1999; Taylor et al., 1995). It is worthy to mention that proteasome complex has the capacity to degrade both sarcoplasmic and myofibrillar proteins, but in an energy-dependent manner (Collins & Goldberg, 2017), which means that the degradation of ubiquitinated proteins by 26S proteasomes requires ATP hydrolysis. In this study and among the 12 common proteins, ubiquitin carboxyl-terminal hydrolase isozyme L3 (UCHL3) as one of the isozymes of ubiquitin *C*-terminal hydrolases with the de-ubiquitinating function, was increasing in abundance by increasing post-mortem time (**Figure 5C**). It is well-known that the ubiquitin system is able to regulate numerous cellular processes such as signal transduction, protein quality control, cell cycle progression, transcriptional regulation, and growth control, and the role of ubiquitination in most of these processes is to promote the degradation of specific proteins (Amerik & Hochstrasser, 2004). The low abundance of UCHL3 early post-mortem could increase protein degradation and fatty acid oxidation, which in turn may play a pivotal role in the

tennderization process. Targeted studies on this UCHL3 and related pathways are needed to better understand its post-mortem roles and relation with meat quality determination.

In this study, we further evidenced for the first time the involvement of ribosomal proteins as another relevant observation in goat post-mortem muscle, signifying that several proteins experiencing changes during storage, also undergo splicing modifications, which is for instance a mechanism known for mitochondrial proteins (Pan, Shai, Lee, Frey, & Blencowe, 2008). This suggests a resilient response of post-mortem muscle cells to energy deprivation (Ubaida-Mohien et al., 2019), essential for energy-demanding cell-death processes such as autophagy and apoptosis (Ouali et al., 2013), both of which were significantly enriched in the goat muscle proteome (**Fig. 6**). Indeed, after slaughter and exsanguination, skeletal muscle cells are confronting hypoxia/ischemia that can induce the activation of apoptosis (Gagaoua, Terlouw, Boudjellal, & Picard, 2015; Longo, Lana, Bottero, & Zolla, 2015). Hallmarks of apoptosis, such as DNA fragmentation, condensation of chromatin, actin degradation, formation of apoptotic bodies as well as activation of caspases are detected in muscles during the post-mortem storage period (Gagaoua, Hafid, et al., 2015; Longo et al., 2015; Ouali et al., 2013).

5. Conclusions

This study revealed important insights regarding the dynamic changes that occur in early post-mortem of goat *Semitendinosus* muscle and particularly, validate the possibility of using specific pathways to analyze/monitor the biological mechanisms underpinning the conversion of muscle into meat. Thanks to the in-depth bioinformatics analyses and a new approach in studying meat tenderization by means of temporal shotgun proteomics, we evidenced for the first time the dynamic time-course changes and molecular signatures underpinning the conversion of goat muscle into meat. Twelve proteins (FHOD1, PDCD6IP, SIRT2, SLC25A3, GPD2, SPR, UCHL3, RPS3A, SGTA, MYOZ2, GSTM3, and NDRG2) were changing in their abundance throughout the storage period, from 1h until 24h post-mortem. Eleven of these proteins are suggested as candidate biomarkers to monitor the changes taking place in the goat muscle proteome during the tenderization phase. In this study, we revealed that energy metabolism and skeletal muscle structure and contraction pathways are significantly involved throughout the early post-mortem period. Moreover, it is interesting to underline that proteins involved in the tricarboxylic acid (TCA) cycle, mitochondrial calcium ion homeostasis, positive regulation of apoptotic process, and autophagy contributed to shed lights on the type of the complex biochemical changes taking place between 1 and 24 h post-mortem in goat muscle. Most of the discussion of this study is

based on studies where animals were slaughtered non-religiously; however, the slaughtering method (religious slaughtering in our case) and differences that can be involved as recently reported for sheep (Kiran et al., 2019), could impact the extent of the differences observed in this trial and thus the interpretation made in terms of muscle-to-meat conversion and muscle proteome changes. Further studies are needed to address this specific question using for instance a shotgun proteomics approach and an adapted trial to capture the similarities and differences.

Acknowledgements

Conflict of interest

No potential conflict of interest was reported by the authors.

CRediT authorship contribution statement

Melisa Lamri: Methodology, Software, Formal analysis, Investigation, Resources, Data curation, Visualization, Writing - original draft. **Antonella della Malva:** Methodology, Software, Formal analysis, Data curation, Visualization, Writing - original draft. Writing – review & editing. **Marzia Albenzio:** Writing - review & editing. **Djamel Djenane:** Writing - review & editing. **Mohammed Gagaoua:** Conceptualization, Methodology, Software, Validation, Formal analysis, Investigation, Resources, Data curation, Visualization, Supervision, Project administration, Funding acquisition, Writing - original draft, Writing - review & editing.

References

Amerik, A. Y., & Hochstrasser, M. (2004). Mechanism and function of deubiquitinating enzymes. *Biochimica et Biophysica Acta (BBA) - Molecular Cell Research, 1695*(1), 189-207. doi: https://doi.org/10.1016/j.bbamcr.2004.10.003

Berchtold, M. W., Brinkmeier, H., & Müntener, M. (2000). Calcium Ion in Skeletal Muscle: Its Crucial Role for Muscle Function, Plasticity, and Disease. *Physiological Reviews, 80*(3), 1215-1265. doi: 10.1152/physrev.2000.80.3.1215

Bjarnadottir, S. G., Hollung, K., Faergestad, E. M., & Veiseth-Kent, E. (2010). Proteome changes in bovine longissimus thoracis muscle during the first 48 h postmortem: shifts in energy status and myofibrillar stability. [Research Support, Non-U.S. Gov't]. *J Agric Food Chem, 58*(12), 7408-7414. doi: 10.1021/jf100697h

Bouley, J., Chambon, C., & Picard, B. (2004). Mapping of bovine skeletal muscle proteins using two-dimensional gel electrophoresis and mass spectrometry. *Proteomics, 4*(6), 1811-1824.

Bradford, M. M. (1976). A rapid and sensitive method for the quantitation of microgram quantities of protein utilizing the principle of protein-dye binding. [Research Support, U.S. Gov't, P.H.S.]. *Anal Biochem, 72*, 248-254.

Cheng, S., Wang, X., Wang, Q., Yang, L., Shi, J., & Zhang, Q. (2020). Comparative analysis of Longissimus dorsi tissue from two sheep groups identifies differentially expressed genes related to growth, development and meat quality. *Genomics, 112*(5), 3322-3330. doi: https://doi.org/10.1016/j.ygeno.2020.06.011

Collins, G. A., & Goldberg, A. L. (2017). The Logic of the 26S Proteasome. *Cell, 169*(5), 792-806. doi: https://doi.org/10.1016/j.cell.2017.04.023

Contreras, L., Drago, I., Zampese, E., & Pozzan, T. (2010). Mitochondria: The calcium connection. *Biochimica et Biophysica Acta (BBA) - Bioenergetics, 1797*(6), 607-618. doi: https://doi.org/10.1016/j.bbabio.2010.05.005

Cross, T. G., Scheel-Toellner, D., Henriquez, N. V., Deacon, E., Salmon, M., & Lord, J. M. (2000). Serine/Threonine Protein Kinases and Apoptosis. *Experimental Cell Research, 256*(1), 34-41. doi: https://doi.org/10.1006/excr.2000.4836

Csapo, R., Gumpenberger, M., & Wessner, B. (2020). Skeletal Muscle Extracellular Matrix – What Do We Know About Its Composition, Regulation, and Physiological Roles? A Narrative Review. [Review]. *Frontiers in Physiology, 11*.

D'Alessandro, A., & Zolla, L. (2013). Meat science: From proteomics to integrated omics towards system biology. *J Proteomics, 78*(0), 558-577. doi: 10.1016/j.jprot.2012.10.023

Dang, D. S., Buhler, J. F., Davis, H. T., Thornton, K. J., Scheffler, T. L., & Matarneh, S. K. (2020). Inhibition of mitochondrial calcium uniporter enhances postmortem proteolysis and tenderness in beef cattle. *Meat Science, 162*, 108039. doi: https://doi.org/10.1016/j.meatsci.2019.108039

Dang, D. S., Stafford, C. D., Taylor, M. J., Buhler, J. F., Thornton, K. J., & Matarneh, S. K. (2022). Ultrasonication of beef improves calpain-1 autolysis and caspase-3 activity by elevating cytosolic calcium and inducing mitochondrial dysfunction. *Meat Science, 183*, 108646. doi: https://doi.org/10.1016/j.meatsci.2021.108646

della Malva, A., Gagaoua, M., Santillo, A., De Palo, P., Sevi, A., & Albenzio, M. (2022). First insights about the underlying mechanisms of Martina Franca donkey meat tenderization during aging: A proteomic approach. *Meat Science, 193*, 108925. doi: https://doi.org/10.1016/j.meatsci.2022.108925

della Malva, A., Maggiolino, A., De Palo, P., Albenzio, M., Lorenzo, J. M., Sevi, A., & Marino, R. (2022). Proteomic analysis to understand the relationship between the sarcoplasmic protein patterns and meat organoleptic characteristics in different horse muscles during aging. *Meat Science, 184*, 108686. doi: https://doi.org/10.1016/j.meatsci.2021.108686

della Malva, A., Santillo, A., Priolo, A., Marino, R., Ciliberti, M. G., Sevi, A., & Albenzio, M. (2023). Effect of hazelnut skin by-product supplementation in lambs' diets: Implications on plasma and muscle proteomes and first insights on the underlying mechanisms. *Journal of Proteomics, 271*, 104757. doi: https://doi.org/10.1016/j.jprot.2022.104757

Di Luca, A., Ianni, A., Bennato, F., Henry, M., Meleady, P., & Martino, G. (2022). A Label-Free Quantitative Analysis for the Search of Proteomic Differences between Goat Breeds. *Animals, 12*(23), 3336.

Ding, Z., Wei, Q., Liu, C., Zhang, H., & Huang, F. (2022). The Quality Changes and Proteomic Analysis of Cattle Muscle Postmortem during Rigor Mortis. *Foods, 11*(2), 217.

England, E. M., Scheffler, T. L., Kasten, S. C., Matarneh, S. K., & Gerrard, D. E. (2013). Exploring the unknowns involved in the transformation of muscle to meat. *Meat Sci, 95*(4), 837-843. doi: 10.1016/j.meatsci.2013.04.031

Fisher, A. B. (2017). Peroxiredoxin 6 in the repair of peroxidized cell membranes and cell signaling. *Archives of Biochemistry and Biophysics, 617*, 68-83. doi: http://dx.doi.org/10.1016/j.abb.2016.12.003

Gagaoua, M., Bonnet, M., De Koning, L., & Picard, B. (2018). Reverse Phase Protein array for the quantification and validation of protein biomarkers of beef qualities: The case of meat color from Charolais breed. *Meat Sci, 145*, 308-319. doi: 10.1016/j.meatsci.2018.06.039

Gagaoua, M., Bonnet, M., Ellies-Oury, M. P., De Koning, L., & Picard, B. (2018). Reverse phase protein arrays for the identification/validation of biomarkers of beef texture and their use for early classification of carcasses. *Food Chemistry, 250*(C), 245-252. doi: 10.1016/j.foodchem.2018.01.070

Gagaoua, M., Duffy, G., Álvarez García, C., Burgess, C., Hamill, R., Crofton, E. C., . . . Troy, D. (2022). Current research and emerging tools to improve fresh red meat quality. *Irish Journal of Agricultural and Food Research*. doi: http://dx.doi.org/10.15212/ijafr-2020-0141

Gagaoua, M., Hafid, K., Boudida, Y., Becila, S., Ouali, A., Picard, B., . . . Sentandreu, M. A. (2015). Caspases and Thrombin Activity Regulation by Specific Serpin Inhibitors in Bovine Skeletal Muscle. *Appl Biochem Biotechnol, 177*(2), 279-303. doi: 10.1007/s12010-015-1762-4

Gagaoua, M., Hughes, J., Terlouw, E. M. C., Warner, R. D., Purslow, P. P., Lorenzo, J. M., & Picard, B. (2020). Proteomic biomarkers of beef colour. *Trends in Food Science & Technology, 101*, 234-252. doi: 10.1016/j.tifs.2020.05.005

Gagaoua, M., Monteils, V., & Picard, B. (2018). Data from the farmgate-to-meat continuum including omics-based biomarkers to better understand the variability of beef tenderness: An integromics approach. *J Agric Food Chem, 66*(51), 13552–13563. doi: 10.1021/acs.jafc.8b05744

Gagaoua, M., & Picard, B. (2022). Chapter 14 - Proteomics to explain and predict meat quality. In P. Purslow (Ed.), *New Aspects of Meat Quality (Second Edition)* (pp. 393-431): Woodhead Publishing.

Gagaoua, M., Schilling, W. M., Zhang, X., & Suman, S. P. (2022). Applications of proteomics in meat research *Reference Module in Food Science*: Elsevier.

Gagaoua, M., Terlouw, E. M. C., Boudjellal, A., & Picard, B. (2015). Coherent correlation networks among protein biomarkers of beef tenderness: What they reveal. *J Proteomics, 128*, 365-374. doi: 10.1016/j.jprot.2015.08.022

Gagaoua, M., Terlouw, E. M. C., Micol, D., Boudjellal, A., Hocquette, J. F., & Picard, B. (2015). Understanding Early Post-Mortem Biochemical Processes Underlying Meat Color and pH Decline in the Longissimus thoracis Muscle of Young Blond d'Aquitaine Bulls Using Protein Biomarkers. *J Agric Food Chem, 63*(30), 6799-6809. doi: 10.1021/acs.jafc.5b02615

Gagaoua, M., Terlouw, E. M. C., Mullen, A. M., Franco, D., Warner, R. D., Lorenzo, J. M., . . . Picard, B. (2021). Molecular signatures of beef tenderness: Underlying mechanisms based on integromics of protein biomarkers from multi-platform proteomics studies. *Meat Sci, 172*, 108311. doi: 10.1016/j.meatsci.2020.108311

Gagaoua, M., Troy, D., & Mullen, A. M. (2021). The Extent and Rate of the Appearance of the Major 110 and 30 kDa Proteolytic Fragments during Post-Mortem Aging of Beef Depend on the Glycolysing Rate of the Muscle and Aging Time: An LC-MS/MS Approach to Decipher Their Proteome and Associated Pathways. *J Agric Food Chem, 69*(1), 602-614. doi: 10.1021/acs.jafc.0c06485

Gagaoua, M., Warner, R. D., Purslow, P., Ramanathan, R., Mullen, A. M., López-Pedrouso, M., . . . Terlouw, E. M. C. (2021). Dark-cutting beef: A brief review and an integromics meta-analysis at the proteome level to decipher the underlying pathways. *Meat Science, 181*, 108611. doi: https://doi.org/10.1016/j.meatsci.2021.108611

Gettins, P. G. (2002). Serpin structure, mechanism, and function. [Research Support, U.S. Gov't, P.H.S. Review]. *Chem Rev, 102*(12), 4751-4804. doi: 10.1021/cr010170+

Goll, D., Neti, G., Mares, S., & Thompson, V. (2008). Myofibrillar protein turnover: the proteasome and the calpains. *Journal of Animal Science, 86*(14_suppl), E19-E35.

Gonçalves, T. M., de Almeida Regitano, L. C., Koltes, J. E., Cesar, A. S. M., da Silva Andrade, S. C., Mourão, G. B., . . . Coutinho, L. L. (2018). Gene Co-expression Analysis Indicates Potential Pathways and Regulators of Beef Tenderness in Nellore Cattle. [Original Research]. *Frontiers in Genetics, 9*. doi: 10.3389/fgene.2018.00441

Gu, M., Wei, Y., Zhang, D., & Liu, Y. (2020). iTRAQ based proteomic profile analysis for goat Longissimus thoracis under repeated freeze-thaw treatments. *LWT, 134*, 109934. doi: https://doi.org/10.1016/j.lwt.2020.109934

Guo, B., Zhang, W., Tume, R. K., Hudson, N. J., Huang, F., Yin, Y., & Zhou, G. (2016). Disorder of endoplasmic reticulum calcium channel components is associated with the increased apoptotic potential in pale, soft, exudative pork. *Meat Science, 115*, 34-40. doi: https://doi.org/10.1016/j.meatsci.2016.01.003

Halper, J., & Kjaer, M. (2014). Basic Components of Connective Tissues and Extracellular Matrix: Elastin, Fibrillin, Fibulins, Fibrinogen, Fibronectin, Laminin, Tenascins and Thrombospondins. In J. Halper (Ed.), *Progress in Heritable Soft Connective Tissue Diseases* (pp. 31-47). Dordrecht: Springer Netherlands.

Han, Z., Chang, C., Zhu, W., Zhang, Y., Zheng, J., Kang, X., . . . Gong, Z. (2021). Role of SIRT2 in regulating the dexamethasone-activated autophagy pathway in skeletal muscle atrophy. *Biochemistry and Cell Biology, 99*(5), 562-569. doi: 10.1139/bcb-2020-0445

Hopkins, D. L., & Ertbjerg, P. (2023). Chapter 12 - The eating quality of meat: II—Tenderness. In F. Toldrá (Ed.), *Lawrie's Meat Science (Ninth Edition)* (pp. 393-420): Woodhead Publishing.

Hopkins, D. L., & Geesink, G. (2009). Protein degradation post mortem and tenderisation. *Applied muscle biology and meat science*, 149-173.

Hopkins, D. L., & Thompson, J. M. (2001). The relationship between tenderness, proteolysis, muscle contraction and dissociation of actomyosin. *Meat Science, 57*(1), 1-12. doi: 10.1016/s0309-1740(00)00065-6

Hou, X., Liu, Q., Meng, Q., Wang, L., Yan, H., Zhang, L., & Wang, L. (2020). TMT-based quantitative proteomic analysis of porcine muscle associated with postmortem meat quality. *Food Chemistry, 328*, 127133. doi: https://doi.org/10.1016/j.foodchem.2020.127133

Hudson, N. J. (2012). Mitochondrial treason: a driver of pH decline rate in post-mortem muscle? *Animal Production Science, 52*(12), 1107. doi: 10.1071/an12171

Hughes, J., Oiseth, S. K., Purslow, P. P., & Warner, R. D. (2014). A structural approach to understanding the interactions between colour, water-holding capacity and tenderness. *Meat Sci, 98*(3), 520-532. doi: 10.1016/j.meatsci.2014.05.022

Ji, C., Liu, J., & Luo, R. (2022). Regulatory role of mitochondrial genes in the tenderisation of lamb meat during postmortem ageing. [https://doi.org/10.1111/ijfs.15678]. *International Journal of Food Science & Technology, 57*(6), 3544-3555. doi: https://doi.org/10.1111/ijfs.15678

Jia, W., Zhang, R., Liu, L., Zhu, Z., Xu, M., & Shi, L. (2021). Molecular mechanism of protein dynamic change for Hengshan goat meat during freezing storage based on high-throughput proteomics. *Food Research International, 143*, 110289. doi: https://doi.org/10.1016/j.foodres.2021.110289

Jia, X., Ekman, M., Grove, H., Faergestad, E. M., Aass, L., Hildrum, K. I., & Hollung, K. (2007). Proteome changes in bovine longissimus thoracis muscle during the early postmortem storage period. [Research Support, Non-U.S. Gov't]. *J Proteome Res, 6*(7), 2720-2731. doi: 10.1021/pr070173o

Jia, X., Hildrum, K. I., Westad, F., Kummen, E., Aass, L., & Hollung, K. (2006). Changes in enzymes associated with energy metabolism during the early post mortem period in longissimus thoracis bovine muscle analyzed by proteomics. *J Proteome Res* (7), 1763-1769. doi: 10.1021/pr060119s

Jia, X., Hollung, K., Therkildsen, M., Hildrum, K. I., & Bendixen, E. (2006). Proteome analysis of early post-mortem changes in two bovine muscle types: M. longissimus dorsi and M. semitendinosis. [Comparative Study
Research Support, Non-U S Gov't]. *Proteomics, 6*(3), 936-944. doi: 10.1002/pmic.200500249

Kemp, C. M., Sensky, P. L., Bardsley, R. G., Buttery, P. J., & Parr, T. (2010). Tenderness--an enzymatic view. [Review]. *Meat Sci, 84*(2), 248-256. doi: 10.1016/j.meatsci.2009.06.008

Kiran, M., Naveena, B. M., Smrutirekha, M., Baswa Reddy, P., Rituparna, B., Praveen Kumar, Y., . . . Rapole, S. (2019). Traditional halal slaughter without stunning versus slaughter with electrical stunning of sheep (Ovis aries). *Meat Science, 148*, 127-136. doi: https://doi.org/10.1016/j.meatsci.2018.10.011

Kiyimba, F., Gagaoua, M., Suman, S. P., Mafi, G. G., & Ramanathan, R. (2022). Bioinformatics: in-depth analyses of omics data in the field of muscle biology and meat biochemistry *Reference Module in Food Science*: Elsevier.

Kwong, J. Q., Davis, J., Baines, C. P., Sargent, M. A., Karch, J., Wang, X., . . . Molkentin, J. D. (2014). Genetic deletion of the mitochondrial phosphate carrier desensitizes the mitochondrial permeability transition pore and causes cardiomyopathy. *Cell Death & Differentiation, 21*(8), 1209-1217. doi: 10.1038/cdd.2014.36

Lamri, M., della Malva, A., Djenane, D., López-Pedrouso, M., Franco, D., Albenzio, M., . . . Gagaoua, M. (2023). Towards the discovery of goat meat quality biomarkers using label-free proteomics. *Journal of Proteomics, 278*, 104868. doi: https://doi.org/10.1016/j.jprot.2023.104868

Lamri, M., Djenane, D., & Gagaoua, M. (2022). Goat meat consumption patterns and preferences in three provinces of Kabylia region in Algeria compared to other meat species: Results of an online survey. *Meat Technology, 63*(2), 96-108.

Lana, A., & Zolla, L. (2015). Apoptosis or autophagy, that is the question: Two ways for muscle sacrifice towards meat. *Trends in Food Science & Technology, 46*(2), 231-241. doi: 10.1016/j.tifs.2015.10.001

Lana, A., & Zolla, L. (2016). Proteolysis in meat tenderization from the point of view of each single protein: A proteomic perspective. [Review]. *Journal of Proteomics, 147*, 85-97. doi: 10.1016/j.jprot.2016.02.011

Laville, E., Sayd, T., Morzel, M., Blinet, S., Chambon, C., Lepetit, J., . . . Hocquette, J. F. (2009). Proteome changes during meat aging in tough and tender beef suggest the importance of apoptosis and protein solubility for beef aging and tenderization. [Research Support, Non-U.S. Gov't]. *J Agric Food Chem, 57*(22), 10755-10764. doi: 10.1021/jf901949r

Lê Cao, K.-A., Boitard, S., & Besse, P. (2011). Sparse PLS discriminant analysis: biologically relevant feature selection and graphical displays for multiclass problems. *BMC Bioinformatics, 12*(1), 253. doi: 10.1186/1471-2105-12-253

Lee, E.-J., Lee, M.-M., Park, S., & Jeong, K.-S. (2022). Sirt2 positively regulates muscle regeneration after Notexin-induced muscle injury. *Experimental and Molecular Pathology, 127*, 104798. doi: https://doi.org/10.1016/j.yexmp.2022.104798

Li, S., & Li, C. (2021). Proteomics discovery of protein biomarkers linked to yak meat tenderness as determined by label-free mass spectrometry. [https://doi.org/10.1111/asj.13669]. *Animal Science Journal, 92*(1), e13669. doi: https://doi.org/10.1111/asj.13669

Liu, M., Wei, Y., Li, X., Quek, S. Y., Zhao, J., Zhong, H., . . . Liu, Y. (2018). Quantitative phosphoproteomic analysis of caprine muscle with high and low meat quality. *Meat Science, 141*, 103-111. doi: https://doi.org/10.1016/j.meatsci.2018.01.001

Lombard, D. B., Tishkoff, D. X., & Bao, J. (2011). Mitochondrial Sirtuins in the Regulation of Mitochondrial Activity and Metabolic Adaptation. In T.-P. Yao & E. Seto (Eds.), *Histone Deacetylases: the Biology and Clinical Implication* (pp. 163-188). Berlin, Heidelberg: Springer Berlin Heidelberg.

Lomiwes, D., Farouk, M. M., Frost, D. A., Dobbie, P. M., & Young, O. A. (2013). Small heat shock proteins and toughness in intermediate pHu beef. *Meat Sci, 95*(3), 472-479. doi: 10.1016/j.meatsci.2013.05.022

Longo, V., Lana, A., Bottero, M. T., & Zolla, L. (2015). Apoptosis in muscle-to-meat aging process: The omic witness. *J Proteomics, 125*(0), 29-40. doi: 10.1016/j.jprot.2015.04.023

López-Pedrouso, M., Lorenzo, J. M., Gagaoua, M., & Franco, D. (2020). Application of Proteomic Technologies to Assess the Quality of Raw Pork and Pork Products: An Overview from Farm-To-Fork. *Biology, 9*(11), 393.

Lum, J. J., Bauer, D. E., Kong, M., Harris, M. H., Li, C., Lindsten, T., & Thompson, C. B. (2005). Growth Factor Regulation of Autophagy and Cell Survival in the Absence of Apoptosis. *Cell, 120*(2), 237-248. doi: https://doi.org/10.1016/j.cell.2004.11.046

Malheiros, J. M., Braga, C. P., Grove, R. A., Ribeiro, F. A., Calkins, C. R., Adamec, J., & Chardulo, L. A. L. (2019). Influence of oxidative damage to proteins on meat tenderness using a proteomics approach. *Meat Sci, 148*, 64-71. doi: 10.1016/j.meatsci.2018.08.016

Matarneh, S. K., Scheffler, T. L., & Gerrard, D. E. (2023). Chapter 5 - The conversion of muscle to meat. In F. Toldrá (Ed.), *Lawrie's Meat Science (Ninth Edition)* (pp. 159-194): Woodhead Publishing.

Mazhangara, I. R., Chivandi, E., Mupangwa, J. F., & Muchenje, V. (2019). The Potential of Goat Meat in the Red Meat Industry. *Sustainability, 11*(13), 3671.

Munekata, P. E. S., Pateiro, M., López-Pedrouso, M., Gagaoua, M., & Lorenzo, J. M. (2021). Foodomics in meat quality. *Current Opinion in Food Science, 38*, 79-85. doi: https://doi.org/10.1016/j.cofs.2020.10.003

Ouali, A. (1990). Meat Tenderization: Possible Causes and Mechanisms. A Review. *Journal of Muscle Foods, 1*(2), 129-165. doi: 10.1111/j.1745-4573.1990.tb00360.x

Ouali, A., Gagaoua, M., Boudida, Y., Becila, S., Boudjellal, A., Herrera-Mendez, C. H., & Sentandreu, M. A. (2013). Biomarkers of meat tenderness: present knowledge and perspectives in regards to our current understanding of the mechanisms involved. *Meat Sci, 95*(4), 854-870. doi: 10.1016/j.meatsci.2013.05.010

Pan, Q., Shai, O., Lee, L. J., Frey, B. J., & Blencowe, B. J. (2008). Deep surveying of alternative splicing complexity in the human transcriptome by high-throughput sequencing. *Nature Genetics, 40*(12), 1413-1415. doi: 10.1038/ng.259

Peña-Blanco, A., & García-Sáez, A. J. (2018). Bax, Bak and beyond — mitochondrial performance in apoptosis. [https://doi.org/10.1111/febs.14186]. *The FEBS Journal, 285*(3), 416-431. doi: https://doi.org/10.1111/febs.14186

Picard, B., & Gagaoua, M. (2020). Meta-proteomics for the discovery of protein biomarkers of beef tenderness: An overview of integrated studies. *Food Res Int, 127*, 108739. doi: 10.1016/j.foodres.2019.108739

Picard, B., Kammoun, M., Gagaoua, M., Barboiron, C., Meunier, B., Chambon, C., & Cassar-Malek, I. (2016). Calcium Homeostasis and Muscle Energy Metabolism Are Modified in HspB1-Null Mice. *Proteomes, 4*(2), 17. doi: 10.3390/proteomes4020017

Purslow, P. P., Gagaoua, M., & Warner, R. D. (2021). Insights on meat quality from combining traditional studies and proteomics. *Meat Sci, 174*, 108423. doi: 10.1016/j.meatsci.2020.108423

Ramanathan, R., Nair, M. N., Wang, Y., Li, S., Beach, C. M., Mancini, R. A., . . . Suman, S. P. (2021). Differential abundance of mitochondrial proteome influences the color stability of beef longissimus lumborum and psoas major muscles. *Meat and Muscle Biology, 5*(1).

Robert, N., Briand, M., Taylor, R., & Briand, Y. (1999). The effect of proteasome on myofibrillar structures in bovine skeletal muscle. *Meat Science, 51*(2), 149-153. doi: https://doi.org/10.1016/S0309-1740(98)00113-2

Rønning, S. B., Andersen, P. V., Pedersen, M. E., & Hollung, K. (2017). Primary bovine skeletal muscle cells enters apoptosis rapidly via the intrinsic pathway when available oxygen is removed. *PLOS ONE, 12*(8), e0182928. doi: 10.1371/journal.pone.0182928

Rossi, D., Pierantozzi, E., Amadsun, D. O., Buonocore, S., Rubino, E. M., & Sorrentino, V. (2022). The Sarcoplasmic Reticulum of Skeletal Muscle Cells: A Labyrinth of Membrane Contact Sites. *Biomolecules, 12*(4), 488.

Schönichen, A., Mannherz, H. G., Behrmann, E., Mazur, A. J., Kühn, S., Silván, U., . . . Geyer, M. (2013). FHOD1 is a combined actin filament capping and bundling factor that selectively associates with actin arcs and stress fibers. *Journal of Cell Science, 126*(8), 1891-1901. doi: 10.1242/jcs.126706

Sentandreu, E., Fuente-García, C., Pardo, O., Oliván, M., León, N., Aldai, N., . . . Sentandreu, M. A. (2021). Protein Biomarkers of Bovine Defective Meats at a Glance: Gel-Free Hybrid Quadrupole-Orbitrap Analysis for Rapid Screening. *Journal of Agricultural and Food Chemistry, 69*(26), 7478-7487. doi: 10.1021/acs.jafc.1c02016

Shang, F., & Taylor, A. (2011). Ubiquitin–proteasome pathway and cellular responses to oxidative stress. *Free Radical Biology and Medicine, 51*(1), 5-16. doi: https://doi.org/10.1016/j.freeradbiomed.2011.03.031

Sierra, V., González-Blanco, L., Diñeiro, Y., Díaz, F., García-Espina, M. J., Coto-Montes, A., . . . Oliván, M. (2021). New Insights on the Impact of Cattle Handling on Post-Mortem Myofibrillar Muscle Proteome and Meat Tenderization. *Foods, 10*(12), 3115.

Sierra, V., & Olivan, M. (2013). Role of mitochondria on muscle cell death and meat tenderization. [Journal article]. *Recent Pat Endocr Metab Immune Drug Discov, 7*(2), 120-129.

Stacklies, W., Redestig, H., Scholz, M., Walther, D., & Selbig, J. (2007). pcaMethods—a bioconductor package providing PCA methods for incomplete data. *Bioinformatics, 23*(9), 1164-1167. doi: 10.1093/bioinformatics/btm069

Tait, S. W. G., & Green, D. R. (2010). Mitochondria and cell death: outer membrane permeabilization and beyond. *Nature Reviews Molecular Cell Biology, 11*(9), 621-632. doi: 10.1038/nrm2952

Taylor, R. G., Tassy, C., Briand, M., Robert, N., Briand, Y., & Cottin, A. (1995). Proteolytic activity of proteasome on myofibrillar structures. *Mol Biol Rep, 21*(1), 71-73. doi: 10.1007/BF00990974

Ubaida-Mohien, C., Lyashkov, A., Gonzalez-Freire, M., Tharakan, R., Shardell, M., Moaddel, R., . . . Ferrucci, L. (2019). Discovery proteomics in aging human skeletal muscle finds change in spliceosome, immunity, proteostasis and mitochondria. *eLife, 8*, e49874. doi: 10.7554/eLife.49874

Wang, L.-L., Han, L., Ma, X.-L., Yu, Q.-L., & Zhao, S.-N. (2017). Effect of mitochondrial apoptotic activation through the mitochondrial membrane permeability transition pore on yak meat tenderness during postmortem aging. *Food Chemistry, 234*, 323-331. doi: https://doi.org/10.1016/j.foodchem.2017.04.185

Wang, Y., Jin, J., Xia, Z., & Chen, H. (2022). miR-363-3p attenuates the oxygen-glucose deprivation/reoxygenation-induced neuronal injury in vitro by targeting PDCD6IP. *Mol Med Rep, 26*(5), 322. doi: 10.3892/mmr.2022.12838

Wang, Z., He, F., Rao, W., Ni, N., Shen, Q., & Zhang, D. (2016). Proteomic analysis of goat Longissimus dorsi muscles with different drip loss values related to meat quality traits. [journal article]. *Food Science and Biotechnology, 25*(2), 425-431. doi: 10.1007/s10068-016-0058-y

Warner, R., Wheeler, T. L., Ha, M., Li, X., Bekhit, A. E.-D., Morton, J., . . . Zhang, W. (2021). Meat tenderness: advances in biology, biochemistry, molecular mechanisms and new technologies. *Meat Science*, 108657. doi: https://doi.org/10.1016/j.meatsci.2021.108657

Wei, Y., Li, X., Zhang, D., & Liu, Y. (2019). Comparison of protein differences between high- and low-quality goat and bovine parts based on iTRAQ technology. *Food Chemistry, 289*, 240-249. doi: https://doi.org/10.1016/j.foodchem.2019.03.052

Wicks, J. C., Bodmer, J. S., Yen, C. N., Zumbaugh, M. D., Matarneh, S. K., Scheffler, T. L., . . . Gerrard, D. E. (2022). Chapter 4 - Postmortem muscle metabolism and meat quality. In P. Purslow (Ed.), *New Aspects of Meat Quality (Second Edition)* (pp. 67-93): Woodhead Publishing.

Wu, S., Luo, X., Yang, X., Hopkins, D. L., Mao, Y., & Zhang, Y. (2020). Understanding the development of color and color stability of dark cutting beef based on mitochondrial proteomics. *Meat Sci, 163*, 108046. doi: 10.1016/j.meatsci.2020.108046

Yang, X., Wu, S., Hopkins, D. L., Liang, R., Zhu, L., Zhang, Y., & Luo, X. (2018). Proteomic analysis to investigate color changes of chilled beef longissimus steaks held under carbon monoxide and high oxygen packaging. *Meat Sci, 142*, 23-31. doi: 10.1016/j.meatsci.2018.04.001

Yu, Q., Tian, X., Shao, L., Xu, L., Dai, R., & Li, X. (2018). Label-free proteomic strategy to compare the proteome differences between longissimus lumborum and psoas major muscles during early postmortem periods. *Food Chemistry, 269*, 427-435. doi: https://doi.org/10.1016/j.foodchem.2018.07.040

Zhai, C., Djimsa, B. A., Prenni, J. E., Woerner, D. R., Belk, K. E., & Nair, M. N. (2020). Tandem mass tag labeling to characterize muscle-specific proteome changes in beef during early postmortem period. *J Proteomics, 222*, 103794. doi: 10.1016/j.jprot.2020.103794

Zhang, J., Ma, D., & Kim, Y. H. B. (2020). Mitochondrial apoptosis and proteolytic changes of myofibrillar proteins in two different pork muscles during aging. *Food Chemistry, 319*, 126571. doi: https://doi.org/10.1016/j.foodchem.2020.126571

Zhang, W., Xiao, S., & Ahn, D. U. (2013). Protein Oxidation: Basic Principles and Implications for Meat Quality. *Critical Reviews in Food Science and Nutrition, 53*(11), 1191-1201. doi: 10.1080/10408398.2011.577540

Zhao, L., Li, F., Zhang, X., Zhang, D., Li, X., Zhang, Y., . . . Wang, W. (2022). Integrative analysis of transcriptomics and proteomics of longissimus thoracis of the Hu sheep compared with the Dorper sheep. *Meat Science, 193*, 108930. doi: https://doi.org/10.1016/j.meatsci.2022.108930

Zhu, Y., Gagaoua, M., Mullen, A. M., Kelly, A. L., Sweeney, T., Cafferky, J., . . . Hamill, R. M. (2021). A Proteomic Study for the Discovery of Beef Tenderness Biomarkers and Prediction of Warner–Bratzler Shear Force Measured on Longissimus thoracis Muscles of Young Limousin-Sired Bulls. *Foods, 10*(5), 952.

Zhu, Y., Gagaoua, M., Mullen, A. M., Viala, D., Rai, D. K., Kelly, A. L., . . . Hamill, R. M. (2021). Shotgun proteomics for the preliminary identification of biomarkers of beef sensory tenderness, juiciness and chewiness from plasma and muscle of young Limousin-sired bulls. *Meat Science, 176*, 108488. doi: 10.1016/j.meatsci.2021.108488

Conflict of interest

No potential conflict of interest was reported by the authors.

CRediT authorship contribution statement

Melisa Lamri: Methodology, Software, Formal analysis, Investigation, Resources, Data curation, Visualization, Writing - original draft. **Antonella della Malva:** Methodology, Software, Formal analysis, Data curation, Visualization, Writing - original draft. Writing – review & editing. **Marzia Albenzio:** Writing – review & editing. **Djamel Djenane:** Writing - review & editing. **Mohammed Gagaoua:** Conceptualization, Methodology, Software, Validation, Formal

analysis, Investigation, Resources, Data curation, Visualization, Supervision, Project administration, Funding acquisition, Writing - original draft, Writing - review & editing.

Figure captions

Fig. 1. Differentially abundant proteins (DAPs) between 1h and 8h post-mortem sampling times in goat *Semitendinosus* muscle. **A)** Volcano plot showing the proteins significantly different (fold change ≥ 1.5 and *P*-value < 0.05) between 1h and 8h post-mortem (details on the full names of the proteins and their molecular functions are given in **Table 1**). The up- and down-regulated proteins at 1h *versus* 8h post-mortem are shown in red and blue, respectively. **B)** Bioinformatics analysis. Bar graph of the 55 DAPs highlighting the functional enrichment analysis using Metascape® (see functional network in **Fig. S1** for further the details). The top 15 enriched and significant Gene Ontology (GO) terms ranked by their *p*-value are given. Stronger colors represent greater significant enrichment. Functional enrichment was performed by selecting Gene Ontology (GO) Biological Processes as ontology source. **C)** Protein-protein interaction analysis of the 55 DAPs using STRING database categorized into eight molecular functions using manual annotations.

Fig. 2. Differentially abundant proteins (DAPs) between 8h and 24h post-mortem sampling times in goat Semitendinosus muscle. **A)** Volcano plot showing the proteins significantly different (fold change ≥ 1.5 and *P*-value < 0.05) between 8h and 24h post-mortem (details on the full names of the proteins and their molecular functions are given in **Table 1**). The up- and down-regulated proteins at 8h *versus* 24h post-mortem are shown in red and blue, respectively. **B)** Bioinformatics analysis. Bar graph of the 52 DAPs highlighting the functional enrichment analysis using Metascape® (see functional network in **Fig. S2** for further the details). The top 13 enriched and significant Gene Ontology (GO) terms ranked by their *p*-value are given. Stronger colors represent greater significant enrichment. Functional enrichment was performed by selecting Gene Ontology (GO) Biological Processes as ontology source. **C)** Protein-protein interaction analysis of the 52 DAPs using STRING database categorized into eight molecular functions using manual annotations.

Fig. 3. Differentially abundant proteins (DAPs) between 1h and 24h post-mortem sampling times in goat Semitendinosus muscle. **A)** Volcano plot showing the proteins significantly different (fold change ≥ 1.5 and *P*-value < 0.05) between 1h and 24h post-mortem (details on the full names of

the proteins and their molecular functions are given in **Table 1**). The up- and down-regulated proteins at 1h *versus* 24h post-mortem are shown in red and blue, respectively. **B**) Bioinformatics analysis. Bar graph of the 154 DAPs highlighting the functional enrichment analysis using Metascape® (see functional network in **Fig. S3** for further the details). The top 20 enriched and significant Gene Ontology (GO) terms ranked by their *p*-value are given. Stronger colors represent greater significant enrichment. Functional enrichment was performed by selecting Gene Ontology (GO) Biological Processes as ontology source. **C**) Protein-protein interaction analysis of the 154 DAPs using STRING database categorized into eight molecular functions using manual annotations (**Table 1**).

Fig. 4. Hierarchical heatmap clustering using the differentially abundant proteins (DAPs) between 1h and 24h post-mortem to compare the enriched Gene Ontology (GO) terms within the up- and down-regulated proteins at 1h post-mortem. Functional enrichment was performed using Metascape® selecting Gene Ontology (GO) Biological Processes as ontology source (further details are given in **Fig. 3**). The heatmap colored by the p-values are indicated by color, where grey cells indicate a lack of significant enrichment in that GO, palest brown indicates a low p-value and darkest brown indicates a high p-value in each of the corresponding post-mortem times. At 1 h post-mortem, only 4 GO terms where enriched from which one "GO:0003018: vascular process in circulatory system" was specific.

Fig. 5. Biological pathway and process enrichment analysis on the total DAPs proteins (n = 174) identified to change early post-mortem among the 3 different time comparisons (1h-8h, 8h-24h and 1h-24h) in the goat *Semitendinosus* muscle. **A**) Circos plot depicting the overlap between proteins changing during early post-mortem time among the three DAPs lists. Proteins that were not differentially abundant are not included. Twelve common proteins (shown with black semi-circles) are changing whatever the post-mortem time comparison and categorized based on the eight molecular functions: i) Binding, transport and calcium homeostasis; ii) Catalytic, metabolism & ATP metabolic process; iii) Proteolysis and associated proteins; iv) Ribosomal proteins; v) Chaperones and/or Heat shock proteins; vi) Muscle contraction, structure and associated proteins including ECM; vii) Oxidative stress, response to hypoxia & cell redox homeostasis; and viii) Miscellaneous. The details on the specific and common proteins (using gene names) of the other conditions are given in **Fig. S4**. **B**) Bar graph showing the biological pathways (top 5 GO terms) found for the 12 common proteins. Functional enrichment was performed using Metascape® selecting Gene Ontology (GO) Biological Processes as ontology source. The bar graphs are colored according to *P*-values: terms with a P-value <0.05, a

minimum count of 2, and an enrichment factor > 1.5. **C**) Protein trajectories of the 12 common proteins for the three post-mortem times defined within the Circos plot. For each individual protein, z-scores were calculated by subtracting the mean normalized protein expression values (relative abundance protein levels) in each condition. **D**) Bi-plot of Principal component analysis (PCA) depicting the separation of the three post-mortem times with the 12 common DAPs proteins. **E**) Heatmap comparing the significantly enriched Gene Ontology (GO) terms using the DAPs proteins of each condition. The heatmap colored by the p-values are indicated by color, where grey cells indicate a lack of significant enrichment in that GO, palest brown indicates a low p-value and darkest brown indicates a high p-value in each of the corresponding post-mortem times. The common GO terms to the three conditions are highlighted by black circles.

Fig. 6. Functional network (related to **Fig. 5C**) constructed with Metascape® depicting the interconnectedness of the GO clusters using the 174 DAPs identified to change over post-mortem time in the goat *Semitendinosus* muscle. The corresponding GO number and the details of the top 20 clusters with their representative enriched terms (one per cluster) are given in the table in the left side of the network ([a] Red (■) refers to 1h-24h; Blue (■) refers to 1h-8h; Green (■) refers to 8h-24h; [b] Percentage to the full protein list that are found in the given ontology term, only input gene names with at least one ontology term annotation are included in the calculation; [c] P-value in log base 10; [d] Multi-test adjusted p-value in log base 10). The most statistically significant term within a cluster is automatically chosen to represent each GO term.

Fig. 7. Proteome changes in goat *Semitendinosus* muscle during the early post-mortem storage period. **A**) Sparse partial least squares-discriminant analysis (sPLS-DA) score plot of goat *Semitendinosus* muscle using the full proteome database showing the extent of discrimination of the goat muscle collected at 1, 8 and 24 h post-mortem. The circles indicate the 95% confidence level. **B**) The loading on component one represents the main 20 proteins behind the separation based on the variable importance in projection. The common proteins changing whatever the post-mortem sampling time are highlighted by yellow arrows. Eleven out of the 12 common proteins were retained in the sPLS-DA analysis, from which five were ranked first.
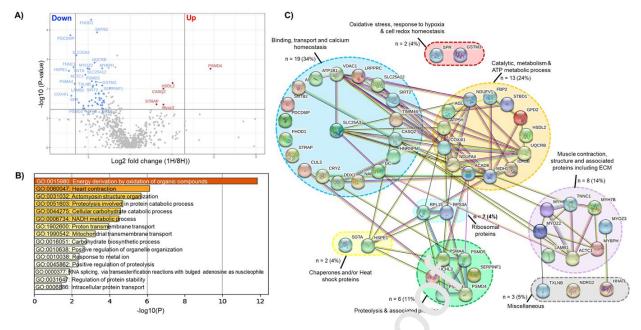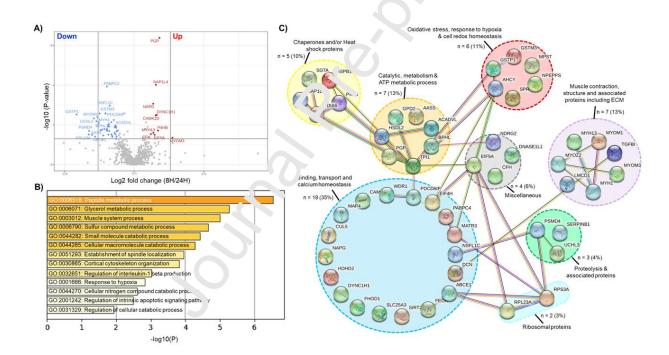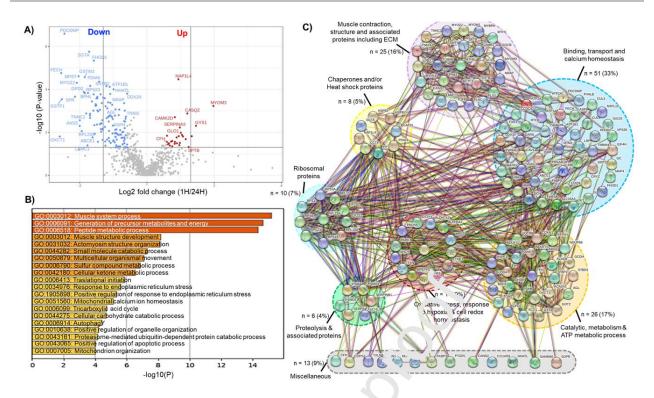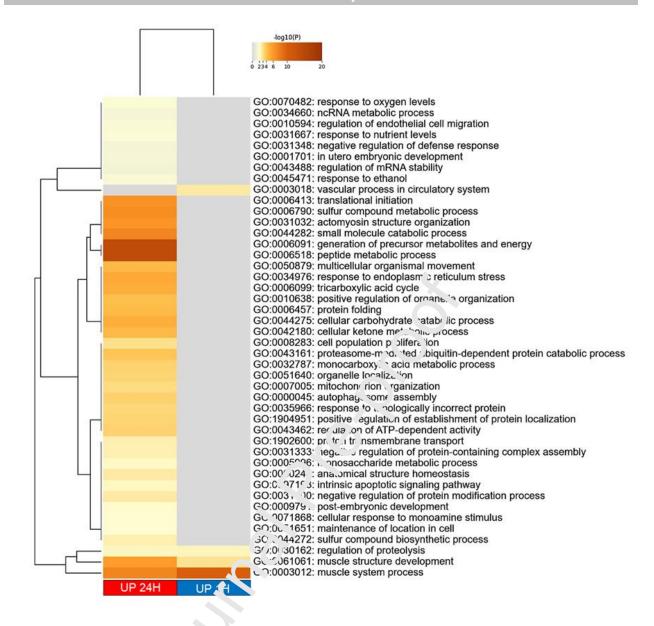
Fig. 1.

Fig. 2.

Fig. 3.

-log10(P)

GO:0070482: response to oxygen levels
GO:0034660: ncRNA metabolic process
GO:0010594: regulation of endothelial cell migration
GO:0031667: response to nutrient levels
GO:0031348: negative regulation of defense response
GO:0001701: in utero embryonic development
GO:0043488: regulation of mRNA stability
GO:0045471: response to ethanol
GO:0003018: vascular process in circulatory system
GO:0006413: translational initiation
GO:0006790: sulfur compound metabolic process
GO:0031032: actomyosin structure organization
GO:0044282: small molecule catabolic process
GO:0006091: generation of precursor metabolites and energy
GO:0006518: peptide metabolic process
GO:0050879: multicellular organismal movement
GO:0034976: response to endoplasmic reticulum stress
GO:0006099: tricarboxylic acid cycle
GO:0010638: positive regulation of organelle organization
GO:0006457: protein folding
GO:0044275: cellular carbohydrate catabolic process
GO:0042180: cellular ketone metabolic process
GO:0008283: cell population proliferation
GO:0043161: proteasome-mediated ubiquitin-dependent protein catabolic process
GO:0032787: monocarboxylic acid metabolic process
GO:0051640: organelle localization
GO:0007005: mitochondrion organization
GO:0000045: autophagosome assembly
GO:0035966: response to topologically incorrect protein
GO:1904951: positive regulation of establishment of protein localization
GO:0043462: regulation of ATP-dependent activity
GO:1902600: proton transmembrane transport
GO:0031333: negative regulation of protein-containing complex assembly
GO:0005996: monosaccharide metabolic process
GO:0060024: anatomical structure homeostasis
GO:0097193: intrinsic apoptotic signaling pathway
GO:0031400: negative regulation of protein modification process
GO:0009791: post-embryonic development
GO:0071868: cellular response to monoamine stimulus
GO:0051651: maintenance of location in cell
GO:0044272: sulfur compound biosynthetic process
GO:0030162: regulation of proteolysis
GO:0061061: muscle structure development
GO:0003012: muscle system process
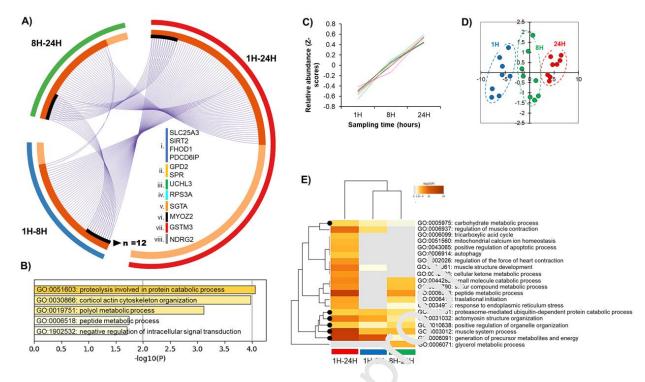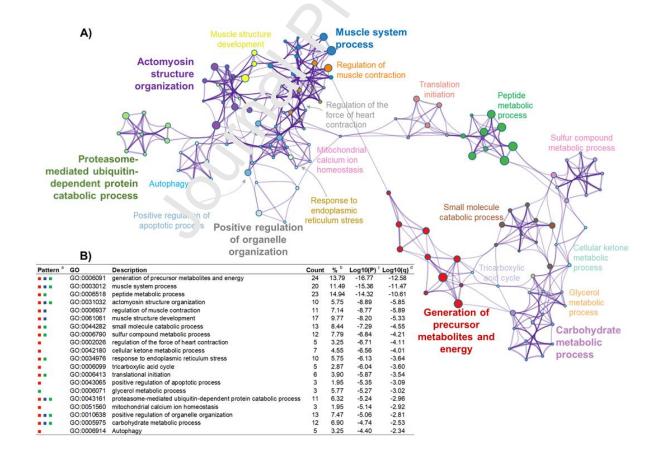
UP 24H   UP 4H

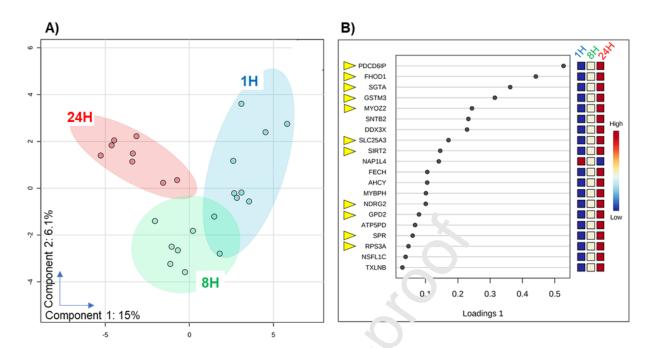**Fig. 4.**

Fig. 5.

Fig. 6.

Fig. 7.

Table 1. List of the differentially abundant proteins (DABs) changing among the three early post-mortem times and organized into eight molecular functions.

Uniprot ID	Full protein names	Gene names	Comparison 1h-8h			Comparison 1h-24h			Comparison 8h-24h		
			FC	log2 (FC)	P-value	FC	log2 (FC)	P-value	FC	log2 (FC)	P-value
Binding, transport and calcium homeostasis (n = 58)											
A0A45 2G5B4	FH1/FH2 domain-containing protein 1	**FHO D1**	0.53	-0.93	4.5 E-05	0.33	-1.58	4.6 E-06	0.64	-0.65	1.4 E-02
A0A45 2GBJ0	Programmed cell death 6-interacting protein	**PDC D6IP**	0.37	-1.42	1.5 E-04	0.18	-2.46	2.5 E-07	0.49	-1.03	2.7 E-03
A0A45 2FAZ4	NAD-dependent protein deacetylase sirtuin-2	**SIRT 2**	0.54	-0.89	8.6 E-03	0.36	-1.48	2.2 E-04	0.67	-0.59	1.9 E-02
A0A45 2G9E1	Phosphate carrier protein, mitochondrial	**SLC2 5A3**	0.41	-1.28	7.3 E-04	0.30	-1.76	1.5 E-04	0.63	-0.66	4.9 E-02
A0A45 2F8U9	ATP-binding cassette sub-family E member 1	ABCE 1				0.33	-1.62	1.7 E-02	0.38	-1.41	3.9 E-02
A0A45 2GAT4	Aspartyl/asparaginyl beta-hydroxylase	ASPH	0.64	-0.64	1.5 E-02	0.62	-0.68	3.0 E-03			
A0A45 2FU58	Sodium/potassium-transporting ATPase subunit beta-1	ATP1 B1	0.60	-0.73	2.4 E-02	0.46	-1.11	7.6 E-05			
A0A45 2E1R1	Calcium/calmodulin-dependent protein kinase type II subunit delta	CAM K2D				1.7	0.83	2.0 E-	1.7	0.77	3.3 E-

Accession	Protein name	Gene	R1	FC1	p-value 1	R2	FC2	p-value 2
(continued from previous page)						8		03 ... 1 ... 03 / 82. ... 1.3
A0A452EKU0	Calsequestrin-2	CASQ2	1.74	0.80	9.8E-03	2.30	1.20	1.3E-03
A0A452EZS5	Quinone oxidoreductase	CRYZ	0.65	-0.62	2.5E-02	0.62	-0.69	2.5E-02
A0A452DVZ8	Cullin-3	CUL3	0.56	-0.83	2.8E-02	0.45	-1.14	3.1E-03
A0A452FUS4	Cullin-5	CUL5	0.67	-0.59	4.9E-02	0.64	-0.64	3.9E-02
A0A452F311	Decorin	DCN	0.52	-0.94	1.6E-02	0.57	-0.82	3.0E-02
A0A452FF51	Eukaryotic translation initiation factor 4H	EIF4H	0.32	-1.64	3.7E-04	0.51	-0.97	2.0E-02
A0A452EST6	Ferrochelatase, mitochondrial	FECH	0.17	-2.55	1.7E-05	0.39	-1.36	6.6E-03
A0A452G129	Vitamin D-binding protein	GC	0.60	-0.74	1.5E-02	0.55	-0.85	1.3E-02
A0A452EST7	Haloacid dehalogenase-like hydrolase domain-containing protein 2	HDHD2	0.46	-1.13	8.6E-03	0.53	-0.93	3.1E-02
A0A452G6T0	Heterogeneous nuclear ribonucleoprotein M	HNRNPM	0.62	-0.69	2.1E-02	0.47	-1.10	1.6E-03
A0A452FES2	Leucine-rich PPR motif-containing protein, mitochondrial	LRPPRC	0.50	-1.00	3.8E-02	0.36	-1.49	4.3E-03
A0A452EJF0	Microtubule-associated protein 4	MAP4	0.46	-1.13	1.7E-03	0.64	-0.65	1.2E-02
A0A452G4H1	Matrin-3	MATR3	0.43	-1.20	2.2E-03	0.58	-0.79	3.6E-02
A0A452G6W6	NSFL1 cofactor p47	NSFL1C	0.40	-1.31	2.4E-04	0.54	-0.88	1.1E-03
A0A452F9K1	Polyadenylate-binding protein 4	PABPC4	0.45	-1.16	4.0E-04	0.51	-0.98	1.2E-04
A0A452FXS6	Beta-2-syntrophin	SNTB2	0.58	-0.79	1.2E-04	0.43	-1.21	7.1E-05
A0A452FXG7	Mitochondrial import inner membrane translocase subunit TIM44	TIMM44	0.46	-1.11	3.8E-02	0.36	-1.48	2.6E-04
A0A452FXM5	Voltage-dependent anion-selective channel protein 1	VDAC1	0.64	-0.64	2.6E-02	0.49	-1.04	5.2E-04
A0A452G510	Vacuolar protein sorting-associated protein 35	VPS35				0.36	-1.46	2.8E-02
A0A452G3B3	14-3-3 protein gamma	YWHAG				0.39	-1.35	3.8E-03

Accession	Protein	Gene			
A0A452G963	Sodium/potassium-transporting ATPase subunit alpha-2	ATP1A2	1.85	0.89	3.2E-02
A0A452E2F6	Alpha-1-acid glycoprotein	AGP	0.42	-1.25	5.6E-03
A0A452FXD0	Sarcoplasmic/endoplasmic reticulum calcium ATPase 1	ATP2A1	0.64	-0.64	1.4E-02
A0A452G1T7	Calcium-transporting ATPase	ATP2A2	0.39	-1.37	9.4E-03
A0A452F8Y4	Caveolin-1	CAV1	1.64	0.72	2.7E-02
A0A452FAV0	Caveolae-associated protein 2	CAVIN2	0.40	-1.31	6.5E-03
A0A452FIW1	PAT complex subunit CCDC47	CCDC47	0.54	-0.88	1.2E-02
A0A452E6J2	Aspartate--tRNA ligase, cytoplasmic	DARS1	0.56	-0.84	1.6E-03
A0A452EQX6	Acyl-CoA-binding protein	DBI	1.77	0.82	3.4E-02
A0A452EXH5	Ubiquinone biosynthesis protein COQ9, mitochondrial	COQ9	0.44	-1.18	2.2E-02
A0A452G0P2	ATP-dependent RNA helicase DDX3X	DDX3X	0.66	-0.59	1.6E-04
A0A452FM00	Fatty acid-binding protein 5	FABP5	2.10	1.07	1.6E-02
A0A452EKA8	Phenylalanine--tRNA ligase beta subunit	FARSB	0.63	-0.66	2.0E-02
A0A452EZC4	RNA-binding protein FXR1	FXR1	0.40	-1.33	2.7E-03
A0A452G2Q3	Glutamine synthetase	GLUL	0.36	-1.48	9.4E-04
A0A452E9Q8	Junctional sarcoplasmic reticulum protein 1	JSRP1	1.84	0.88	1.7E-02
A0A452G069	WD repeat-containing protein 1	WDR1	0.52	0.96	1.2E-02
A0A452FYW6	Cytoplasmic dynein 1 heavy chain 1	DYNC1H1	1.76	0.81	3.1E-03
A0A452E9T4	Guanine nucleotide-binding protein G(s) subunit alpha isoforms short	GNAS1	0.49	-1.04	1.9E-03
A0A452EYC7	Myotubularin	MTM1	0.45	-1.14	1.8E-02
A0A452	ATP-dependent RNA helicase DDX1	DDX1	0.	-	1.4

2E6Q6			0.59	0.75	10^{-2}						
A0A452FTQ1	Alpha-soluble NSF attachment protein	NAPA	0.51	-0.97	2.7×10^{-2}						
A0A452DKZ3	Gamma-soluble NSF attachment protein	NAPG							1.61	0.68	8.6×10^{-4}
A0A452FSH7	cAMP-dependent protein kinase type II-alpha regulatory subunit	PRKAR2A	0.52	-0.96	2.9×10^{-2}						
A0A452G043	Parvalbumin alpha	PVALB	0.59	-0.76	1.8×10^{-2}						
A0A452GA81	RNA-splicing ligase RtcB homolog	RTCB	0.47	-1.09	4.2×10^{-4}						
A0A452DTX3	Electrogenic aspartate/glutamate antiporter SLC25A12, mitochondrial	SLC25A12	0.51	-0.97	2.1×10^{-2}						
A0A452FME4	Serine-threonine kinase receptor-associated protein	STRAP	1.55	0.65	$3.\times 10^{-2}$						
A0A452FMJ8	Synaptopodin-2	SYNPO2	2.51	1.33	1.5×10^{-2}						
A0A452FKN8	Transketolase	TKT	1.57	0.65	3.2×10^{-2}						
Catalytic, metabolism & ATP metabolic process (n = 30)											
A0A452F334	Glycerol-3-phosphate dehydrogenase, mitochondrial	GPD2	0.54	-0.90	3.7×10^{-2}	0.27	-1.88	1.3×10^{-4}	0.51	-0.98	1.6×10^{-2}
A0A452E108	Alpha-aminoadipic semialdehyde synthase, mitochondrial	AASS				0.25	-2.00	5.0×10^{-3}	0.35	-1.52	3.2×10^{-2}
A0A452E8J9	Isobutyryl-CoA dehydrogenase, mitochondrial	ACAD8	0.63	-0.68	1.2×10^{-2}	0.44	-1.18	7.6×10^{-4}			
A0A452G2D9	Very long-chain specific acyl-CoA dehydrogenase, mitochondrial	ACADVL				0.49	-1.02	2.4×10^{-3}	0.60	-0.73	5.7×10^{-3}
A0A452EMK6	Glycogen debranching enzyme	AGL	0.63	-0.67	3.0×10^{-2}	0.52	-0.94	8.5×10^{-4}			
A0A452G5E3	ATP synthase subunit d, mitochondrial	ATP5PD	0.65	-0.62	1.5×10^{-2}	0.47	-1.09	1.6×10^{-4}			
A0A452F5X7	Valacyclovir hydrolase	BPHL				0.28	-1.85	1.5×10^{-4}	0.41	-1.28	7.8×10^{-3}
A0A452F0R5	Fructose-1,6-bisphosphatase isozyme 2	FBP2	0.63	-0.67	4.5×10^{-2}	0.52	-0.93	1.6×10^{-2}			
A0A452E1U5	Hydroxysteroid dehydrogenase-like protein 2	HSDL2	2.02	1.01	6.3×10^{-3}				0.63	-0.68	1.1×10^{-2}
A0A452E8M7	Isocitrate dehydrogenase [NAD] subunit beta, mitochondrial	IDH3B	0.65	-0.62	2.9×10^{-2}	0.57	-0.80	1.3×10^{-2}			
A0A45…	Cytochrome b-c1 complex subunit 7	UQC…	0.	-	1.3	0.	-	1.3			

Accession	Protein name	Gene	Value	±	Ratio	p-value	Value	±	Ratio	p-value	Value	±	Ratio	p-value
2EHX9		RB	0.56		0.85	1.7E-03	0.59		0.77	1.3E-02				
A0A452EEG7	Cytochrome c oxidase subunit 4 isoform 1, mitochondrial	COX4I1	0.38	-	1.40	2.4E-02	0.29	-	1.81	2.7E-03				
A0A452FQM6	NADH dehydrogenase [ubiquinone] flavoprotein 1, mitochondrial	NDUFV1	0.53	-	0.91	2.0E-02	0.42	-	1.24	9.6E-02				
A0A452EA11	Starch-binding domain-containing protein 1	STBD1	0.60	-	0.74	7.0E-02	0.61	-	0.70	1.9E-03				
A0A452ET55	Triosephosphate isomerase	TPI1					0.39	-	1.37	7.0E-03	0.43	-	1.21	1.9E-02
A0A452DUT2	Cytoplasmic aconitate hydratase	ACO1					0.66	-	0.59	9.8E-02				
A0A452G711	D-beta-hydroxybutyrate dehydrogenase, mitochondrial	BDH1					0.60	-	0.74	4.0E-03				
A0A452DPQ1	Fumarate hydratase, mitochondrial	FH					0.53	-	0.91	4.5E-02				
A0A452DVV2	Glutaryl-CoA dehydrogenase, mitochondrial	GCDH					1.56	-	0.84	2.5E-02				
A0A452EG24	Aspartate aminotransferase, mitochondrial	GOT2					1.68	-	0.75	5.0E-02				
A0A452F0W1	Glycogen [starch] synthase, muscle	GYS1					2.74	-	1.46	5.0E-03				
A0A452EQW7	Malate dehydrogenase, cytoplasmic	MDH1	0.56	-	0.82	1.5E-02								
A5JSS3	Cytochrome c oxidase subunit NDUFA4	NDUFA4	0.63	-	0.66	3.6E-02								
A0A452EKC1	NADH dehydrogenase [ubiquinone] 1 beta subcomplex subunit 8	NDUFB8					0.62	-	0.68	4.9E-02				
A0A452FXF1	NADH dehydrogenase [ubiquinone] iron-sulfur protein 2, mitochondrial	NDUFS2					0.39	-	1.35	4.3E-04				
A0A452EAK6	Succinyl-CoA:3-ketoacid coenzyme A transferase 1, mitochondrial	OXCT1					0.17	-	2.60	1.6E-02				
A0A452EB05	Pyruvate dehydrogenase E1 component subunit beta, mitochondrial	PDHB					0.45	-	1.15	1.9E-03				
D3K382	Protein disulfide-isomerase A3	PDIA3					0.38	-	1.40	4.2E-03				
A0A452EJU5	Glycerol-3-phosphate phosphatase	PGP									1.88	-	0.91	4.2E-07
A0A452G830	Prostaglandin reductase 1	PTGR1					0.65	-	0.63	1.8E-03				
Muscle contraction, structure and associated proteins including ECM (n = 29)														
T1RLJ2	Myozenin-2	**MYO**	0.	-		2.0	0.	-		4.9	0.	-		1.6

Accession	Protein	Gene									
		Z2	50	1.01	E-03	24	2.09	E-05	47	1.08	E-02
A0A452DQP6	Actin, alpha cardiac muscle 1	ACTC1	0.48	-1.07	3.3E-03	0.42	-1.26	2.6E-04			
A0A452G534	Laminin subunit beta-1	LAMB1	0.45	-1.14	8.7E-03	0.38	-1.40	9.0E-04			
A0A452F0M9	Myosin-binding protein H	MYBPH	0.63	-0.67	2.0E-03	0.43	-1.23	6.1E-04			
A0A452F6C9	Myosin-1	MYH1				0.33	-1.59	9.8E-04	0.40	-1.32	4.1E-03
A0A452EZH4	Myosin-6	MYH6	0.47	-1.09	4.6E-02	0.35	-1.53	5.8E-04			
A0A452EJS4	Myomesin-1	MYOM1				0.33	-1.51	5.4E-04	0.42	-1.24	2.7E-03
A0A452DWY7	Myomesin-3	MYOM3				3.93	1.98	5.9E-04	2.60	1.38	4.4E-02
A0A452DR88	Transforming growth factor-beta-induced protein ig-h3	TGFBI				0.51	-0.96	1.1E-02	0.54	-0.90	1.2E-02
F6KVT2	Troponin C, slow skeletal and cardiac muscles	TNNC1	0.03	-1.35	1.8E-03	0.25	-2.00	2.7E-03			
A0A452FH25	Filamin-C	FLNC				2.22	1.15	2.1E-02			
A0A452EL69	Laminin subunit gamma-1	LAMC1				0.29	-1.77	4.1E-02			
A0A452E1G1	LIM domain-binding protein 3	LDB3				0.47	-1.08	3.1E-02			
A0A452EDZ9	LIM and cysteine-rich domains protein 1	LMCD1							0.46	-1.11	3.4E-02
A0A452E9W0	Myosin-13	MYH13							1.61	0.69	2.5E-02
A0A452FDI1	Myosin-14	MYH14				1.54	0.63	3.6E-02			
A0A452F3X0	Myosin-7B	MYH7B	0.62	-0.70	3.6E-02						
A0A023IYH7	Myozenin-3	MYOZ3	1.74	0.80	3.4E-02						
A0A452FDI6	Nebulin-related-anchoring protein	NRAP				0.62	-0.68	4.3E-04			
A0A452F6N4	Plastin-3	PLS3				0.64	-0.64	4.9E-02			
A0A452G4T8	Beta-sarcoglycan	SGCB				0.5	-0.91	7.3E-			

Accession	Protein	Gene	Ratio	Fold	p-value	Ratio	Fold	p-value	Ratio	Fold	p-value
			3		E-03						
A0A452DPE6	Smoothelin-like protein 1	SMTNL1	0.57	-0.80	4.5E-02						
A0A452G859	Beta-1-syntrophin	SNTB1	1.78	0.83	2.8E-02						
A0A452E729	Spectrin beta chain, erythrocytic	SPTB	2.36	1.24	4.8E-02						
A0A452EVX3	Troponin I, slow skeletal muscle	TNNI1	0.50	-1.01	2.5E-02						
W8G3C9	Troponin I, fast skeletal muscle	TNNI2	0.63	-0.66	9.7E-04						
A0A452F0K7	Tropomyosin alpha-3 chain	TPM3	1.59	0.68	4.1E-02						
A0A452FRG1	Tubulin alpha-8 chain	TUBA8	0.52	-0.93	5.0E-02						
A0A452DLF4	Vinculin	VCL	0.49	-1.03	1.1E-02						
Oxidative stress, response to hypoxia & cell redox homeostasis (n = 15)											
A0A452E0A7	Glutathione S-transferase Mu 3	**GSTM3**	0.57	-0.82	5.8E-03	0.28	-1.85	2.7E-05	0.49	-1.04	2.6E-03
A0A452FWA7	Sepiapterin reductase	**SPR**	0.43	-1.22	2.9E-02	0.23	-2.14	2.2E-04	0.50	-1.00	1.7E-02
A0A452F7N2	Adenosylhomocysteinase	AHCY	0.35	-1.50	2.6E-04	0.52	-0.94	1.0E-02			
A0A452EJW7	Glutathione S-transferase P	GSTP1	0.17	-2.53	2.9E-04	0.24	-2.07	3.0E-03			
A0A452G9M2	3-mercaptopyruvate sulfurtransferase	MPST	0.24	-2.04	2.5E-05	0.58	-0.78	3.9E-02			
A0A452FQK2	Puromycin-sensitive aminopeptidase	NPEPPS	0.48	-1.06	1.8E-03	0.57	-0.82	7.2E-03			
A0A452FEB8	Succinate-semialdehyde dehydrogenase, mitochondrial	ALDH5A1	0.46	-1.12	2.6E-02						
A0A452DWP9	Alpha-aminoadipic semialdehyde dehydrogenase	ALDH7A1	0.52	-0.94	1.1E-02						
A0A452ED36	B-cell receptor-associated protein 31	BCAP31	1.93	0.95	1.5E-02						
A0A452EI23	Persulfide dioxygenase ETHE1, mitochondrial	ETHE1	0.64	-0.64	2.3E-03						
A0A452F4X9	Lactoylglutathione lyase	GLO1	2.01	1.00	1.0E-02						
A0A452F9C0	Glutathione S-transferase omega-2	GSTO2	0.66	-0.67	3.2E-						

Accession	Protein	Gene	Val 1		Ratio 1	p 1	Val 2		Ratio 2	p 2	Val 3		Ratio 3	p 3
							3			02				
A0A452FM54	Parkinson disease protein 7	PARK7					0.60	-	0.73	1.8E-02				
A0A452EUX2	Peroxiredoxin-6	PRDX6					0.63	-	0.66	6.3E-03				
A0A452EGP3	Thioredoxin	TXN					0.63	-	0.66	3.1E-03				

Ribosomal proteins (n = 10)

Accession	Protein	Gene	Val 1		Ratio 1	p 1	Val 2		Ratio 2	p 2	Val 3		Ratio 3	p 3
A0A452EVI7	40S ribosomal protein S3a	**RPS3A**	0.57	-	0.82	2.0E-02	0.35	-	1.53	4.9E-04	0.61	-	0.71	2.5E-02
A0A452ELX4	60S ribosomal protein L15	RPL15	0.59	-	0.77	3.4E-02	0.58	-	0.80	7.9E-03				
A0A452F945	60S ribosomal protein L23a	RPL23A					0.62	-	1.94	8.8E-03	0.32	-	1.64	3.0E-02
A0A452E6F8	Eukaryotic translation initiation factor 2 subunit 1	EIF2S1					0.40	-	1.32	2.2E-02				
A0A452E855	40S ribosomal protein S6	RPS6					0.31	-	1.70	1.6E-03				
A0A452DXK9	40S ribosomal protein S23	RPS23					0.31	-	1.69	6.8E-05				
A0A452E9F4	Eukaryotic translation initiation factor 2 subunit 2	EIF2S2					0.63	-	0.67	1.7E-02				
A0A452G5D5	60S ribosomal protein L10a	RPL10A					0.52	-	0.95	1.7E-03				
A0A452GB27	40S ribosomal protein S11	RPS11					2.06	-	1.04	1.3E-02				
A5JST6	40S ribosomal protein S18	RPS18					0.31	-	1.69	1.4E-03				

Proteolysis & associated proteins (n = 9)

Accession	Protein	Gene	Val 1		Ratio 1	p 1	Val 2		Ratio 2	p 2	Val 3		Ratio 3	p 3
A0A452F429	Ubiquitin carboxyl-terminal hydrolase isozyme L3	**UCHL3**	0.57	-	0.80	7.3E-03	0.31	-	1.69	2.1E-03	0.37	-	1.45	4.7E-03
A0A452EAB1	Proteasome subunit alpha type-4	PSMA4	0.40	-	1.32	6.7E-03	0.34	-	1.57	4.6E-03				
A0A452FI84	26S proteasome non-ATPase regulatory subunit 5	PSMD5	0.53	-	0.91	5.5E-03	0.53	-	0.92	1.1E-02				
A0A452G3P7	26S proteasome non-ATPase regulatory subunit 4	PSMD4	3.78	-	1.92	2.1E-03					0.32	-	1.62	2.0E-02
A0A452F5G1	Leukocyte elastase inhibitor	SERPINB1					0.50	-	1.01	4.8E-03	0.53	-	0.91	9.0E-03
A0A452G7E7	Pigment epithelium-derived factor	SERPINF1					0.63	-	0.66	7.7E-03	0.56	-	0.83	8.7E-04

Accession	Protein name	Gene	Ratio	$\log_2$	p-value	Ratio	$\log_2$	p-value	Ratio	$\log_2$	p-value
A0A452DZU0	Alpha-1-antichymotrypsin	SERPINA3	1.97	0.98	5.9E-03						
A0A452EWR7	Proteasome subunit alpha type-3	PSMA3	1.97	0.98	3.1E-02						
A0A452DQ02	26S proteasome non-ATPase regulatory subunit 3	PSMD3	0.46	-1.12	4.6E-02						
Chaperones and/or Heat shock proteins (n = 9)											
A0A452G497	Small glutamine-rich tetratricopeptide repeat-containing protein alpha	**SGTA**	0.50	-1.01	2.1E-03	0.30	-1.72	1.8E-06	0.61	-0.71	1.3E-02
A0A452ESU7	Heat shock protein beta-1	HSPB1				0.39	-1.37	3.8E-03	0.45	-1.16	1.7E-02
A0A452E0C3	10 kDa heat shock protein, mitochondrial	HSPE1	0.36	-1.46	2.4E-03	0.42	-1.24	4.1E-02			
A0A452EXC0	Nucleosome assembly protein 1-like 4	NAP1L4				1.91	0.93	3.4E-05	1.72	0.78	9.7E-05
A0A452DVG8	Protein disulfide-isomerase A6	PDIA6	0.37	-1.42	4.3E-05	0.64	-0.64	2.1E-02			
A0A452EJT8	T-complex protein 1 subunit delta	CCT4	0.40	-1.32	7.5E-03						
A0A452ETE8	T-complex protein 1 subunit zeta	CCT6A	0.52	-0.95	7.6E-03						
A0A452G662	Heat shock protein beta-7	HSPB7	0.37	-1.45	1.1E-03						
A0A452G7V5	Protein disulfide-isomerase	P4HB							1.81	0.86	1.9E-02
Miscellaneous (n = 14)											
A0A452EAY4	Protein NDRG2	**NDRG2**	0.58	-0.79	3.1E-02	0.33	-1.59	1.7E-04	0.63	-0.67	3.0E-02
A0A452FF76	Complement factor H	CFH				1.51	0.60	1.4E-02	1.51	0.60	2.9E-02
A0A452FSE0	Protein-cysteine N-palmitoyltransferase HHAT-like protein	HHATL	0.64	-0.64	4.8E-02	0.50	-0.99	9.9E-05			
A0A452G9A6	Beta-taxilin	TXLNB	0.54	-0.88	7.8E-03	0.38	-1.38	1.7E-04			
A0A452FBU0	eIF5-mimic protein 2	BZW1	0.34	-1.55	1.2E-02						
A0A452F2J8	Cullin-associated NEDD8-dissociated protein 2	CAND2	0.50	-1.00	2.4E-02						
A0A452FJG6	COP9 signalosome complex subunit 2	COPS2	1.51	0.59	2.8E-02						
A0A45…	Peptidyl-prolyl cis-trans isomerase	FKBP	1.…	0.75	4.5E-0…						

Accession	Protein name	Gene	FC	r	p-value	FC	r	p-value
2F711	FKBP3	3	6.8		3.9E-02			
A0A452ED39	Glutamine amidotransferase-like class 1 domain-containing protein 3	GATD3A	1.95	0.96	3.6E-02			
A0A452DZ71	Glyoxalase domain-containing protein 4	GLOD4	0.61	-0.72				
A0A452FH30	Deoxyribonuclease-1-like 1	DNASE1L1				0.54	-0.90	2.0E-02
A0A452G2G2	Eukaryotic translation initiation factor 5A-1	EIF5A				1.66	0.73	3.2E-02
A0A452FVK2	Sorting and assembly machinery component 50 homolog	SAMM50	0.54	-0.88	4.9E-02			
A0A452G1L9	Protein-glutamine gamma-glutamyltransferase 2	TGM2	2.54	-0.90	2.2E-02			

The proteins in bold correspond to the common proteins whatever the comparison (post-mortem time).

Table 2. Total number of protein identified (and percentage) among the three early post-mortem times categorized into eight molecular functions

Molecular functions/pathways	All times	1h-8h	8h-24h	1h-24h
Total number of DAPs proteins	174	55	52	153
Binding, transport and calcium homeostasis	58 (33%)	19 (34%)	18 (35%)	51 (33%)
Catalytic, metabolism & ATP metabolic process	30 (17%)	13 (24%)	7 (13%)	26 (17%)
Muscle contraction, structure and associated proteins including ECM	29 (17%)	8 (14%)	7 (13%)	25 (16%)
Oxidative stress, response to hypoxia & cell redox homeostasis	15 (9%)	2 (4%)	6 (11%)	14 (9%)
Ribosomal proteins	10 (6%)	2 (4%)	2 (4%)	10 (7%)
Chaperones and/or Heat shock protein	9 (5%)	2 (4%)	5 (10%)	8 (5%)
Proteolysis & associated proteins	9 (5%)	6 (11%)	3 (6%)	6 (4%)
Miscellaneous	14 (8%)	3 (5%)	4 (8%)	13 (9%)

The color gradients, within each color, are added to highlight the dynamic changes over times and protein counts differences among the three pairwise comparisons.

Highlights

- First study of the temporal changes in early post-mortem proteome of goat *Semitendinosus* muscle

- Shotgun proteomics revealed 174 differentially abundant proteins from interconnected pathways
- Proteomics profiling of early post-mortem muscle offers an unparalleled view of the biochemical events underlying muscle into meat conversion
- Energy metabolism and muscle structure are significant pathways
- Pivotal role of energy production and mitochondrial metabolism in muscle into meat conversion